In vivo and in vitro studies of polyetheretherketone: bone formation, inflammatory response and biofilm formation

Sargon Barkarmo

Department of Prosthodontics/Dental Materials Science
Institute of Odontology
Sahlgrenska Academy at University of Gothenburg

UNIVERSITY OF GOTHENBURG

Gothenburg 2019

Cover illustration by Johan Thompson

In vivo and in vitro studies of polyetheretherketone:
bone formation, inflammatory response and biofilm formation

sargon.barkarmo@odontologi.gu.se

ISBN 978-91-7833-298-4 (PRINT)
ISBN 978-91-7833-299-1 (PDF)

http://hdl.handle.net/2077/58494

Printed by BrandFactory in Gothenburg, Sweden 2019

To my family

ܐ ܟܬܒ ܒܐܘ ܚܫܚܐ ܡܢ ܡܢܢܐ. ܐܘ ܟܝ ܒܐܬܗܐ ܟܬܘܗ.
ـ ܡܚܟܘܐ ܬܟܘ ܩܠܐܒ

"If you wish to distinguish that which is sweet from that which is sour,
you owe it to yourself to try both."

Naum Palak, Assyrian writer

In vivo and in vitro studies of polyetheretherketone: bone formation, inflammatory response and biofilm formation

Sargon Barkarmo

Department of Prosthodontics/Dental Materials Science, Institute of Odontology
Sahlgrenska Academy, University of Gothenburg
Gothenburg, Sweden

ABSTRACT

In prosthetic dentistry, restorative materials are used to replace missing teeth and tissues, so as to maintain oral functionalities and comfort for the patient. Depending on the clinical problem, metals, ceramics or polymers, are used both in dentistry and orthopedics. The present thesis focuses on the polymer material polyetheretherketone (PEEK), which has been used in orthopedic applications for about 30 years, mainly as a component of spinal devices - as such it has provided good clinical outcomes. PEEK has recently been adopted as part of dental rehabilitation owing to its many favorable properties, including high-level mechanical strength, chemical resistance, and biocompatibility. Therefore, it is of interest and important to extend our basic understanding of PEEK as a material that can be used in various prosthetic devices. Moreover, it is important to investigate whether modifications made to the surface of the material generate outcomes that may be translated to prosthetic dentistry, thereby using PEEK as a more broadly applicable dental material.

The overall aim of this thesis was to use in vivo and in vitro experimental methods to investigate the potential of PEEK as a material for use in dental devices.

In vivo studies were conducted to investigate the host bone responses to cylinder shaped and threaded PEEK implants that were coated with nanocrystalline hydroxyapatite (nanoHA), as compared to uncoated control implants. The results revealed significantly higher mean values for the biomechanical and histomorphometric parameters for the nanoHA PEEK, as compared to the control material.

The levels of cytokines expressed by peripheral blood mononuclear cells (PBMCs) when exposed in vitro to PEEK, blasted PEEK, and titanium 6-aluminum 4-vanadium (Ti6Al4V) were investigated at different time-points. The PBMCs produced significantly higher levels of pro-inflammatory cytokines when exposed to the PEEK surface than when exposed to the Ti6Al4V surface. The blasted PEEK surface induced the highest level of pro-inflammatory cytokine release from the PBMCs.

The ability to form a biofilm in vitro was assessed by inoculating oral bacterial species onto PEEK, blasted PEEK, commercially pure titanium (cp-Ti), and Ti6Al4V. Biofilm formation was quantified after staining with crystal violet. The blasted PEEK showed increased biofilm formation by *S. sanguinis*, *S. oralis* and *S. gordonii* as compared to the other surfaces, while the levels of bacterial adhesion to PEEK, cp-Ti, and Ti6Al4V were similar.

It appears that nanoHa-coated, threaded PEEK implants improve bone formation, as compared to uncoated PEEK implants, and that PEEK induces a stronger inflammatory response than does Ti6Al4V. The biofilm formation results suggest that the level of bacterial adhesion to PEEK is similar to that of cp-Ti and Ti6AlV4.

Within the limitations of the methods used in the present thesis, it can be concluded that PEEK may have potential as a material for use in various dental applications.

Keywords: PEEK, polyetheretherketone, hydroxyapatite, nanotopography, osseointegration, cytokines, biofilms, biomaterials, dental materials, titanium, nanocoated.

ISBN 978-91-7833-298-4 (PRINT) http://hdl.handle.net/2077/58494
ISBN 978-91-7833-299-1 (PDF)

SAMMANFATTNING PÅ SVENSKA

Vid rehabiliterande tandvård används olika implantat och proteser för att ersätta förlorade tänder och vävnad så att patienter kan upprätthålla funktion och estetik. För att materialen ska kunna fungera över lång tid behöver de inneha vissa egenskaper. Polyetheretherketon (PEEK) är en relativt ny polymer som har visat sig kunna vara lämplig för att användas kliniskt. Hittills har PEEK använts framförallt inom ortopedi men intresset för detta material har på senare tid ökat inom odontologi. Det är väsentligt att studera detta material och huruvida man kan förändra dessa egenskaper för att förbättra dess funktion.

Det huvudsakliga syftet med avhandlingen var att vetenskapligt studera olika aspekter på hur väl PEEK fungerar som ett biomaterial.

I de två första in vivo studierna undersöktes benbildningen till PEEK genom att belägga ytan med ett bioaktivt ämne (nanoHA) med förhoppning om att stimulera benbildningen till implantat. Resultaten visade högre biomekaniska data och mer benkontakt för PEEK implantat belagda med nano-HA jämförd med kontrollgruppen.

Den inflammatoriska reaktionen till PEEK, blästrad PEEK och titanium-6 aluminum-4-vanadium (Ti6Al4V) undersöktes genom att mäta cytokinutsöndringen av immunceller i kontakt med de olika materialen. Resultaten visade att immuncellerna i kontakt med PEEK utsöndrade mer proinflammatoriska cytokiner jämfört med Ti6Al4V medan den blästrade PEEK ytan framkallade den högsta andelen proinflammatoriska cytokiner.

Tillväxt av biofilm av olika orala bakterie jämfördes mellan PEEK, blästrad PEEK, kommersiellt rent titan (cp-Ti) och Ti6Al4V. Resultaten visade ökad tillväxt av *S. sanguinis*, *S. oralis* och *S. gordonii* på blästrade PEEK medan biofilm tillväxten var likvärdig för oblästrad PEEK, cp-Ti och Ti6Al4V.

Sammantaget visade resultaten att benbildningen ökade genom att belägga gängade PEEK implantat med nano partiklar av hydroxylapatit. PEEK framkallade en starkare inflammatorisk reaktion jämfört med titanlegering och att orala bakterier växer på PEEK-ytor i motsvarande mängd som på titan och titanlegering.

Inom studiens begränsning så är sammanfattning att PEEK, i vissa fall, kan vara ett alternativ att användas i olika konstruktioner inom protetisk tandvård.

LIST OF PAPERS

This thesis is based on the following studies, which are referred to in the text by their Roman numerals.

I. Barkarmo S, Wennerberg A, Hoffman M, Kjellin P, Breding K, Handa P, Stenport V. **Nano-hydroxyapatite-coated PEEK implants: a pilot study in rabbit bone.** *J Biomed Mater Res A. 2013 Feb;101(2):465-71. doi: 10.1002/jbm.a.34358.*

II. Barkarmo S, Andersson M, Currie F, Kjellin P, Jimbo R, Johansson CB, Stenport V. **Enhanced bone healing around nanohydroxyapatite-coated polyetheretherketone implants: An experimental study in rabbit bone.** J *Biomater Appl. 2014 Nov;29(5):737-47. doi: 10.1177/0885328214542854.*

III. Barkarmo S, Östberg AK, Johansson CB, Franco-Tabares S, Johansson PH, Dahlgren U, Stenport V. **Inflammatory cytokine release from human peripheral blood mononuclear cells exposed to polyetheretherketone and titanium-6 aluminum-4 vanadium in vitro.** *J Biomater Appl. 2018 Aug;33(2):245-258. doi: 10.1177/0885328218786005.*

IV. Barkarmo S, Longhorn D, Leer K, Johansson CB, Stenport V, Franco-Tabares S, Kuehne S, Sammons R. **Biofilm formation on PEEK and Titanium surfaces**. *Manuscript Submitted.*

CONTENT

ABBREVIATIONS

AFM	Atomic force microscopy
BA	Bone area
BIC	Bone-to-implant contact
BHI	Brain Heart Infusion medium
Cfu	Colony-forming units
Cp-Ti	Commercially pure titanium
DAPI	4′,6-diamidino-2-phenylindole
EDX	Energy-dispersive x-ray spectroscopy
ELI	Extra low interstitials
FBGC	Foreign body giant cell
G-CSF	Granulocyte colony-stimulating factor
GRO	Growth-regulated oncogene
HA	Hydroxyapatite
HGF	Hepatocyte growth factor
IFN	Interferon
IL	Interleukin
MI	Mirror image
MIG	Monokine induced by interferon gamma
MNGC	Multinucleated giant cell
NanoHA	Nanocrystalline hydroxyapatite
NGF	Nerve growth factor
PEEK	Polyetheretherketone
PBMC	Peripheral blood mononuclear cell
PBS	Phosphate-buffered saline
PFA	Paraformaldehyde
PMMA	Polymethylmethacrylate
PMN	Polymorphonuclear leukocyte
ROI	Region of interest
RTQ	Removal torque
SCGF	Stem cell growth factor
SDF	Stromal cell-derived factor
SEM	Scanning electron microscopy
TBS	Tris-buffered saline
Ti6Al4V	Titanium-6 aluminum-4 vanadium
TNF	Tumor necrosis factor
UHMWPE	Ultra-high-molecular-weight polyethylene
XPS	X-ray photoelectron spectroscopy

1 INTRODUCTION

Polyetheretherketone (PEEK) is a polymer that is used as a surgical material in orthopedic spinal implants, as well as in dental applications owing to its many favorable properties, which include mechanical strength, chemical resistance, and biocompatibility. Already since its biocompatibility was confirmed in the 1980s, there has been considerable interest in the field of biomaterials research in the potential of PEEK for clinical applications.

In the introduction to a handbook on PEEK (1) it is stated that: '*PEEK biomaterials are currently used in thousands of spinal fusion patients around the world every year. Durability, biocompatibility and excellent resistance to aggressive sterilization procedures make PEEK a polymer of choice, replacing metal in orthopedic implants, from spinal implants and hip replacements to finger joints and dental implants.'.*

The concept of a 'biomaterial' was introduced by Williams in 1987 as *'A nonviable material used in a medical device intended to interact with biological systems'* (2). A more specific definition provided by the American National Institutes of Health is: '*any substance or combination of substances, other than drugs, synthetic or natural in origin, which can be used for any period of time, which augments or replaces partially or totally any tissue, organ or function of the body, in order to maintain or improve the quality of life of the individual*'(3).

Biomaterials are usually in the forms of metals, ceramics, and polymers. Polymeric biomaterials are currently used extensively in medical applications, especially in regenerative tissue engineering. Since the chemical architectures of synthetic polymers share similarities with natural tissues, proteins, and polysaccharides, it has been suggested that polymers are more authentic mimics of natural tissues than are metals and ceramics (4). Drug delivery agents, sutures, membranes, and load-bearing implants, to name a few polymers, are used in medicine.

While metallic biomaterials are frequently used for hard tissue applications, they have certain drawbacks, such as stress shielding, wear particles, cytotoxicity, and allergenicity (5, 6).

Restorative materials are used in prosthetic dentistry to replace missing teeth and tissues, so as to maintain oral functionalities and to ensure comfort and desired appearance. Polymers are fundamental to restorative dentistry and are

used in a wide-variety of applications, as cavity-filling materials (i.e., 'composites'), cements, and materials in fixed and removable dentures. Polymers can be processed with "simple" methods at low cost. They are esthetically pleasing and possess physical properties that are suitable for the oral cavity (7). However, cytotoxic residual monomers can leak out from denture materials into the saliva and cause allergic reactions (8, 9).

The majority of oral implants currently in use are composed of commercially pure titanium (cp-Ti) grade 4, while several dental prosthetic components are manufactured from titanium alloys, such as titanium-6 aluminum-4 vanadium (Ti6Al4V), which has superior mechanical properties to cp-Ti (10). However, the polymer PEEK, with its suitable mechanical and biocompatible properties, is attracting interest as a material for dental devices, and it may in some cases replace the metal components using in the dental field.

1.1 MATERIAL PROPERTIES

PEEK used as a biomaterial has been reviewed extensively by Kurtz and Devine, who describe in detail the mechanical properties of PEEK-containing materials (11). To summarize, PEEK is a semi-crystalline, thermoplastic polymer with a stable chemical structure. It is formed by stepwise polymerization and is composed of repeating units of the monomer etheretherketone (Figure 1). The rigidity of the repeating units of phenyl groups offers excellent physical and chemical properties. PEEK is usually processed by standard thermoplastic techniques, such as extrusion, injection molding or machining into desired forms and sizes for use in medical applications. The crystalline content of PEEK is dependent upon the manufacturing process but is usually in the range of 30%–35%. This high degree of crystallinity also contributes to the mechanical strength of PEEK.

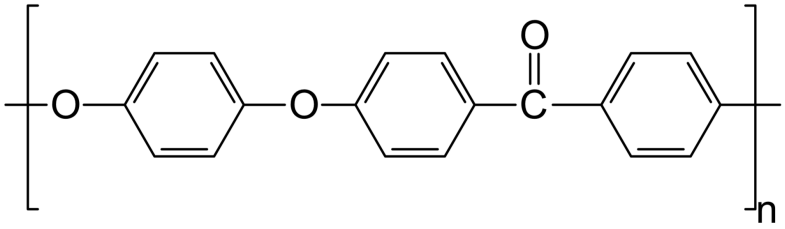

Figure 1. Chemical structure of PEEK. Source: Gardner 1998 (12).

As mentioned above, PEEK is a strong material with favorable mechanical properties that can be augmented through the incorporation of carbon fibers (13). While unfilled PEEK has an elastic modulus of 3–4 GPa, with carbon fiber reinforcement (CFR) it can match that of cortical bone (18 GPa) (Figure 2). Using PEEK with an elastic modulus that is in the same range as cortical bone reduces the risk of stress shielding around the implant and makes it suitable for use in orthopedic and spinal surgeries (14). The tensile strength of unfilled PEEK has been reported to be approximately 100 MPa, as compared to 60 MPa for polymethylmethacrylate (PMMA) (Figure 2).

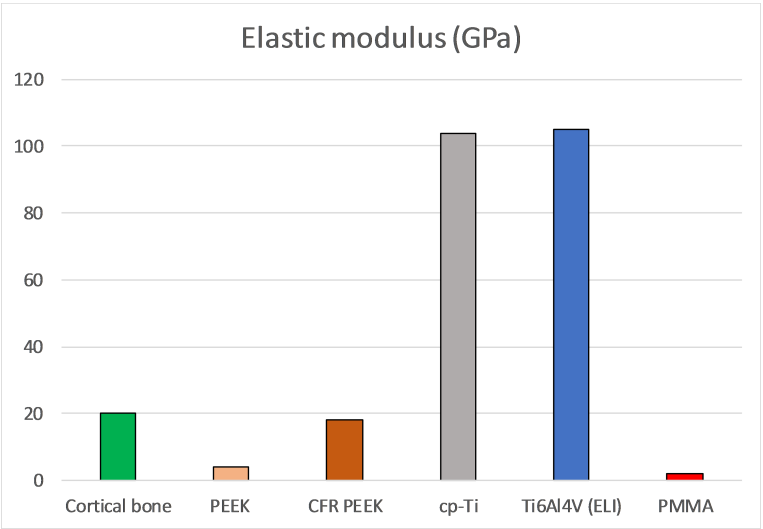

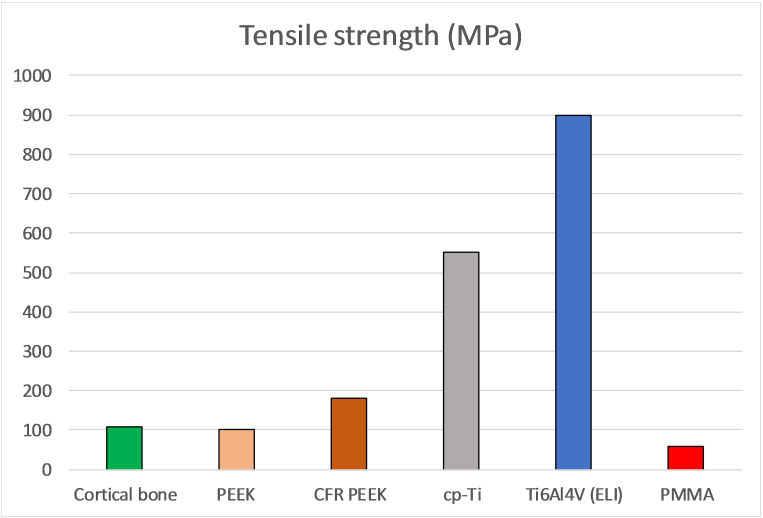

Figure 2. Elastic modulus (upper) and tensile strength (lower) values for cortical bone (15), PEEK (16), and CFR-PEEK (17), Cp-Ti (10), Ti6Al4V (ELI) (10), and PMMA (7). The data are obtained from different sources, references are given within the parentheses.

From the mechanical perspective, PEEK is also appropriate as a restorative material in dental applications, such as fixed and removable dentures (18). In a study carried out by Scwitalla et al., the flexural modulus (i.e., the capacity to resist bending) and the flexural strength (i.e., the ability to resist deformation under load) of 11 different PEEK compounds were tested using a three-point bending test (19). The samples were tested "dry" and also after incubation at 37°C in Ringer's solution for 1, 7, 28 and 84 days. The flexural modulus values ranged from 2.73 GPa for unfilled PEEK up to 47.27 GPa for CFR-PEEK, while the respective flexural strength values ranged from 170.37 MPa to 1009.63 MPa. The duration of incubation seemed to have a negligible effect on the outcomes. Even the lower flexural values considerably exceeded the minimum strength of 50 MPa required for polymer-based crown and bridge materials according to ISO 10477:2018 (20).

The stable chemical structure of PEEK makes it unreactive and resistant to degradation. For example, PEEK is insoluble in all conventional solvents, with the exception of concentrated sulfuric acid (21). Even though PEEK is not impaired by long-term exposure to water, it has been shown that water adsorption can reduce the crystallinity of PEEK (22). However, others have shown that the mechanical properties were unchanged when PEEK was tested in saline in a cyclic compression fatigue experiment (23).

PEEK has a glass transition temperature in the range of 143°–160°C, and a melting temperature in the range of 335°–441°C (11). PEEK is also thermally stable and is not degraded even at temperatures exceeding 300°C (24). Thermal degradation at body temperature is therefore not considered to be an issue for clinical applications. Furthermore, sterilization by steam autoclaving does not affect the physical properties of PEEK (25). PEEK also remains stable when exposed to gamma radiation, which is an advantage when sterilizing polymer medical devices (26).

The radiolucency of PEEK facilitates radiographic examinations of implants in bone tissues (27). In contrast, metallic implants can produce artifacts in computer tomography and magnetic resonance imaging, making it difficult to interpret the status of the bone tissues surrounding the implants (28). However, to improve the contrast visualization of PEEK (e.g., in spinal implants), it is possible to add, for example, barium sulfate to the material (1).

1.2 BIOCOMPATIBILITY

The initial definition of biocompatibility proposed by Williams in 1987 was as follows: '*Biocompatibility refers to the ability of a material to perform with an appropriate host response in a specific application'* (29).

This definition focused on the aspects of the material. However, this rather general definition of biocompatibility has been refined over the years, such that nowadays various definitions exist that include the complex interactions that occur between the material and the host tissues.

The term 'biocompatibility' has mostly been used to describe the response of the material to the tissue with which it comes in contact. However, as the tissue may influence the biomaterial and the biomaterial may influence the tissue, another definition of biocompatibility was suggested by Williams in 1999:

'*Biocompatibility is a two-way process that evolves over time, with host affecting the material and material affecting the host'* (30).

Albrektsson and coworkers listed the following six factors that they consider to influence the tissue response to an implant (31):

1. Implant material
2. Implant design
3. Implant surface
4. Status of the host tissue
5. Surgical technique
6. Loading conditions

Depending on the "hard factors" (factors 1-3) and the "soft factors" (factors 4-6) involved, it is currently difficult to put forward a precise definition of biocompatibility. Considering the various definitions that exist in the literature, one can only state that biocompatibility is a 'living definition'. For more information on this topic, the interested readers are referred to the publication by Williams in 2014, titled '*There is no such thing as a biocompatible material'* (32). The latter paper is of interest because it argues that *'biocompatibility is a perfectly acceptable term, but that it subsumes a variety of mechanisms of interaction between biomaterials and tissues or tissue components and can only be considered in the context of the characteristics of both the material and the biological host within which it placed'*.

In vitro and in vivo studies have been conducted that have investigated the biocompatibility features of PEEK biomaterials. The cytotoxicity and mutagenesis of PEEK were evaluated by Katzer et al in two in vitro tests (33). In one test, strains of *Salmonella typhimurium* were incubated with PEEK and in a second test, fibroblasts from hamsters were grown on PEEK. The results from both tests showed no evidence of cytotoxic or mutagenic effects of PEEK, which is an important requirement for a biomaterial.

The biocompatibility of PEEK has also been investigated in other animal models. Jockish and coworkers inserted CFR-PEEK into rabbit muscle for 8–12 weeks. The authors reported no adverse tissue responses or infections related to the PEEK implant (34).

Direct bone contact (i.e., osseointegration) with PEEK implants has also been examined in animal studies. For example, implants of PEEK in the rabbit femur and tibia have been shown to be well-integrated, as confirmed by histomorphometry and biomechanical tests (35, 36). In a study conducted by Toth and colleagues, contacts between bone and PEEK material have been observed in interbody spinal implants in sheep (37). However, these implants were partially surrounded by fibrous tissue, suggesting that the PEEK itself has low osteoconductive properties, which could lead to weak osseointegration. Therefore, there is interest in improving the biocompatibility of PEEK through surface modifications.

Comparing PEEK to titanium

While bone formation and osseointegration around cp-Ti (grade 1–4) implants have been clearly demonstrated, the tissue responses to PEEK have not been investigated as extensively. When comparing PEEK to titanium, in different in vitro and in vivo experimental models, it appears that the bone response to uncoated PEEK is inferior to the corresponding response to titanium. For example, an in vitro study has shown a stronger angiogenic response (which is important for bone formation) to a titanium alloy than to PEEK (38). In a clinical study, titanium (the grade of which unfortunately was not specified) and PEEK interbody lumbar cages for spinal fusion were implanted in patients. Radiographic evaluations showed significantly higher bone fusion to the titanium than to the PEEK at 2 years postimplantation (39). The lower level of bone formation around PEEK might be attributable to the formation of fibrous tissue rather than bone tissue, as reported for PEEK implants in vivo (37). The formation of soft tissue around PEEK has been suggested to be the result of more potent inflammatory responses to PEEK than to Ti6Al4V (40). Mesenchymal cells cultured on PEEK had higher levels of mRNA species for factors associated with apoptosis, while rough Ti6Al4V promoted osteoblastic

differentiation, which favors bone formation (40). In a systematic review, the osseointegrative capabilities of PEEK and titanium used as dental implants were compared (41). Although there have been only a few studies, it has been concluded that the osseointegration properties of PEEK are inferior to those of titanium.

1.3 SURFACE MODIFICATIONS

As mentioned above, PEEK in its pure form has limitations regarding its osseointegration into bone tissues (37). Therefore, researchers have focused on techniques to modify the implant surface so as to improve the osteoconductive capacity of PEEK. Incorporating bioactive materials into the polymer (42) and changing the surface properties (43) represent two strategies for achieving this.

According to Hench and coworkers, a bioactive material is defined as a material that has the capacity to bond to a living tissue (44). Various bioactive materials have been described in the literature, including hydroxyapatite (HA) (45), bisphosphonate (46), insulin (47), and laminin (48). It has been suggested that these bioactive materials, when coated onto implants, contribute to a rapid biochemical bonding between the implant and the bone tissue (49).

It has been proposed that a surface that has low energy, such as PEEK, experiences decreased protein adsorption (50). Fibronectin, which is a protein that is important for cell adhesion, exhibits a favorable orientation on a hydrophilic surface. Consequently, alteration of the surface energy could lead to improved adhesion of osteoblasts to the surface, resulting in enhanced integration into bone (51, 52). The chemical composition and the roughness of the surface are two features that can be modified to promote bone healing (53). This can be achieved, for example, by coating the surface with titanium, which is a well-documented material for promoting osseointegration (54). An in vitro study has shown that the maturation of osteoblasts adherent to Ti6Al4V is increased compared to osteoblasts adherent to PEEK (38). Enhanced bone formation has also been shown in vivo on PEEK surfaces coated with titanium, as compared to uncoated PEEK (55). In another study, the osseointegration of a sandblasted PEEK implant with a micro-rough surface was compared to that of mirror-polished PEEK (56). The implants were inserted in rat femurs and were investigated with a pull-out test after 2 and 4 weeks of healing. Significantly higher pull-out force was shown for the rougher, sandblasted implants, suggesting improved osseointegration compared to the smoother, mirror-polished PEEK implants.

Another method to improve bone healing, as mentioned earlier, is to apply a coating with osteoconductive properties (such as HA) to the surface of the PEEK (43, 57-59). Due to its similarity to the mineral phase of natural bone tissue, artificial HA has been used for several decades as a bioactive coating material (60, 61) and has been shown to enhance on osseointegration when coated onto implants (62).

Several techniques are available to apply HA coatings to PEEK surfaces. For example, surface modifications have been generated through plasma spray deposition of HA (43, 63) and spin coat deposition of a thin layer of nanocrystalline HA (nanoHA) (64).

Some concerns have been raised regarding the thickness of the HA coating on PEEK, and studies using coatings with thicknesses >10 μm have revealed complications with regard to the detachment of the coating from the bulk material (65, 66). To avoid detachment, a technique for applying a thinner, more stable, nanometer-thick, coating has been developed (67, 68). Surface topography influences the bone responses not only at the micrometer level, but also at the nanometer level of the implants (69). Titanium implants coated with nanometer-sized HA particles have shown enhancement of early bone formation in vivo (67). Even though the effect on osteogenesis at the cellular level has not been fully clarified, it has been suggested that the nanometer-sized particles facilitate adhesion of osteoblasts to the implant surface, thereby accelerating bone formation (70-72).

The beneficial impact on bone healing around nanocrystalline hydroxyapatite (nanoHA)-coated implants has been proposed to be due to a synergistic effect of surface nanotopography and altered chemistry (73, 74).

1.4 INFLAMMATION

During surgical implant insertion, tissue trauma occurs, which immediately initiates an inflammatory host response. Regardless of tissue type, this early inflammation plays a central role in the integration and functionality of the implant.

Immunity is usually divided into the innate and adaptive systems. The innate immune system mounts rapid and non-specific responses and represents an important primary defense mechanism against foreign bodies, while the adaptive immune system is a secondary host defense system that is more specialized, using lymphocytes to identify specific antigens and generating antibodies (75). The inflammatory response and the integration of biomaterials

have been described in terms of an innate immune reaction that involves neutrophils and macrophages (76).

Macrophage activation can result in classical (M1) or alternative (M2) phenotypes (77). The classically activated M1 macrophages are phagocytic and kill microorganisms, while M2 macrophages are involved in wound healing and repair (75). The different pathways of activation of macrophages rely on the secretion of cytokines (77). The M1 macrophages are triggered by lipopolysaccharide (LPS) or interferon (IFN)-γ that is released by T helper 1 (Th1) cells. The wound-healing M2 macrophages are instead activated by interleukin (IL)-4, which is produced by eosinophils, basophils, and Th2 cells (77). In a study conducted by Omar et al., monocytes were activated either classically (M1) or alternatively (M2) and then the cells were cultured on anodically oxidized or machined titanium surfaces (78). It was shown that the classically activated monocytes communicated pro-osteogenic signals to human mesenchymal stem cells, which can promote bone healing. However, the different surface properties seemed to exert weak effects on the osteogenic signal from the monocytes.

The complex series of events that occurs after implant insertion is described in detail in excellent reviews by Franz and colleagues (79) and Anderson and colleagues (80), respectively. In essence, when a material comes in contact with a tissue the immune system is affected by the biomaterial that will initiate the wound healing. Blood proteins are adsorbed to the surface of the material, which leads to activation of the coagulation cascade, complement system, and innate immune cells. The immune cells that initially migrate from the blood towards the implant in the acute inflammatory phase are mostly polymorphonuclear leucocytes (PMNs, granulocytes). These PMNs are involved in the acute inflammatory response and they secrete chemokines that attract other leukocytes, such as monocytes, to the implant-tissue interface. Pro-inflammatory cytokines, such as IL-4 and tumor necrosis factor-α (TNF-α), play important roles in the acute inflammation (see Table 1). A couple of days after implant insertion, the PMNs disappear and the mononuclear cells (monocytes and lymphocytes) appear at the implant site. As the chronic phase develops, the monocytes differentiate into macrophages, which in turn secrete chemokines. In the presence of a foreign material, these chemokines will promote the fusion of macrophages to form foreign body giant cells (FBGCs) (81). FBGCs, also termed multinucleated giant cells (MNGCs), are associated with bone-biomaterial integration (82).

As mentioned above, the macrophages in proximity to the implant surface play important roles in wound healing and tissue regeneration (83). The cytokines

that are induced during the implantation process can also influence the actions of the macrophages. For example, IL-4 induces macrophage fusion to form FBGCs (or MNGCs) (84). This host reaction to a foreign material is the end-stage of the inflammatory and the early wound-healing responses that arise during the implantation of a biomaterial (80).

The surface properties are known to influence the tissue responses and the functions of the biomaterial (69). It has also been shown that the release of pro-inflammatory cytokines, such as IL-1β, IL-6, and TNF-α, is related to specific material surface properties, and that both surface chemistry and surface morphology influence the release of these cytokines (85).

The release of various cytokines and growth factors in response to contact with different biomaterials provides information regarding the inflammatory responses to such materials, thereby enhancing our understanding of the complexity of the early tissue responses.

Table 1. Cytokines associated in wound-healing and inflammatory responses to biomaterials.

Cytokine	Function
IL-1β	Facilitates the adhesion of leukocytes to the endothelial surface by increasing the numbers of adhesion receptors. Produced by pro-inflammatory M1 macrophages that are exposed to LPS or IFN-γ. Associated with osteolysis. (86-88)
IL-4	Proliferation of B lymphocytes and T-helper cells. Stimulates the formation of M2 macrophages. Induces the formation of FBGCs. (77, 84, 88)
IL-6	Has both pro-inflammatory and anti-inflammatory activities. Stimulates the differentiation of T and B cells. Regulates osteoblast and osteoclast development. (88-90)
IL-10	An anti-inflammatory cytokine that inhibits the secretion of pro-inflammatory cytokines from macrophages and Th1 cells. Inhibits osteoclast formation. (88, 91, 92)
TNF-α	Produced by macrophages and is a major pro-inflammatory cytokine. Involved in bone remodeling and plays an important role in bone-related diseases. Prevents the apoptosis of monocytes. (93-95)
IFN-γ	Released by Th1 cells. Activates M1 macrophages, upregulates pro-inflammatory cytokines, and inhibits anti-inflammatory cytokines. (77)

Wear particles

In the case of load-bearing implants, there is a concern regarding the debris produced through wear of the implant material, especially in total joint arthroplasties. These wear particles can induce osteolysis and cause implant failure (96). A similar problem exists for the particles released in conjunction with dental implants (97). Titanium particles have been identified in the peri-implant soft tissue (98), and ion release of titanium has been detected in bone tissues proximal to the implants (99). Although the reason why particles are released around dental implants is not clear, several events have been implicated, such as particle release during implant insertion (100), wear at the implant-abutment level (101), and corrosion (102). In orthopedic research, it has been shown that particle size, as well as the composition, morphology, and concentration of the material are factors that correlate with cytokine release from macrophages (103). The activated macrophages release pro-inflammatory mediators, such as IL-1β, IL-6, and TNF-α, which can cause osteolysis (104). Particle release from dental implants have, therefore, been suggested to aggravate inflammation and may be the reason for the occurrence of peri-implantitis (98).

Hallab et al. have shown that macrophages exposed to PEEK (particle sizes of 0.7 μm, 2 μm, and 10 μm) for 24 hours or 48 hours exhibit significantly lower levels of release of pro-inflammatory cytokines, as compared to macrophages exposed to ultra-high-molecular-weight polyethylene (UHMWPE) (87). The UHMWPE particles were more cytotoxic than the PEEK particles, with the 0.7-μm UHMWPE particles showing the highest levels of cytotoxicity. The authors of that study suggested that a stronger inflammatory response to the implant material might have negative consequences in the clinical setting, given that pro-inflammatory cytokines can disrupt bone homeostasis. It was concluded that PEEK particles are more biocompatible than UHMWPE particles (87). The biologic responses to PEEK-related wear debris from total joint arthroplasties have been summarized in a systematic review (105). The results from the reviewed studies are inconsistent when considering inflammatory cytokine release. Therefore, it is important to investigate further the early inflammatory responses to PEEK, especially since it is being considered as a replacement material for other polymers and metals in various clinical applications.

PBMCs

Human peripheral blood mononuclear cells (PBMCs) comprise lymphocytes (T cells, B cells, NK cells), monocytes, and dendritic cells. These cells are often used to study biocompatibility and inflammation (88). Applying this in vitro model with PBMCs, one can determine the inflammatory responses to

various materials, since PBMCs produce a wide array of cytokines. This information will be of importance when choosing biomaterials for different clinical applications. Although in vitro methods have inherent limitations and cannot be compared to the in vivo situation, they are important tools for screening biomaterials and increasing our understanding of the basic cellular responses to such biomaterials.

1.5 BACTERIAL BIOFILMS

Biofilms are microorganisms that co-aggregate on a surface to form a colony that is usually enclosed within an extracellular polymeric matrix (106). Biomaterials in the oral cavity are generally not sequestered within the tissue but are instead exposed to the saliva with varying pH levels, as well as to a wide variety of bacteria. More than 700 bacterial species have been detected in the oral environment (107), and biofilms are formed on all exposed surfaces, including the materials used in restorative applications (108).

The process of biofilm formation can be divided into three stages: attachment, colonization, and biofilm development (109). To survive in the oral cavity, bacteria must adhere to pellicle-coated surfaces, desquamating surfaces or to bacteria that are already surface-bound (110). During attachment, the initial colonizers utilize the pellicle generated by the saliva conditioning film and express surface receptors that facilitate their adherence (111). Primary colonizers include various streptococcal species, such as *Streptococcus sanguinis*, *Streptococcus gordonii*, and *Streptococcus oralis*, all of which can adhere directly to the surface and bind to other species already present in the nascent biofilm (112).

Biofilms exists in healthy individuals and are usually harmless, consisting predominantly of commensal bacteria. However, if these biofilms are allowed to expand, their composition may change, allowing pathogens to become more prevalent (113). Depending on the location of the biofilm in the mouth, caries and gingivitis (and subsequently, periodontitis or peri-implantitis) may occur. Some pathogens, for example *Enterococcus faecalis,* have been shown to be highly resistant to a range of antibiotics (114). Therefore, it is important to use biomaterials that do not enhance biofilm formation.

The factors that determine the levels of bacterial growth on different restorative materials are not well understood. Some studies have shown that biofilm formation on metals differs from that on ceramics and polymers (115). In addition to the chemical composition and surface free energy, the presence and dimensions of surface features, such as pores and defects, which can create

favorable conditions for bacterial growth, may also influence bacterial adhesion (113). Hahnel et al. compared the formation of multispecies biofilms on different abutment materials in vitro (116). They showed that biofilm formation on PEEK was similar to or weaker than that on zirconia or titanium. However, the surface of the PEEK material used in Hahnel's study was significantly smoother than the zirconia and titanium surfaces. The smoother surface may have influenced the result, since other studies have shown that an increase in surface roughness significantly favors bacterial attachment and biofilm formation and facilitates biofilm growth (117, 118).

Most studies of bacterial growth on PEEK have focused on pathogens associated with orthopedic infections, such as *Staphylococcus aureus*, *Staphylococcus epidermidis*, *Pseudomonas aeruginosa* and *Escherichia coli* (119, 120). Increased knowledge of bacterial adhesion and biofilm formation on novel materials will improve our understanding regarding their applications and the potential risk of developing disease. However, apart from the study conducted by Hahnel et al., there is little information in the literature on the adhesion and proliferation of oral bacteria to PEEK (116).

1.6 CLINICAL APPLICATIONS

As mentioned earlier, PEEK is used extensively in orthopedic and spinal surgery applications. However, it is also used as a material in a number of other devices that are employed in medical and dental rehabilitation (121). For example, PEEK fusion cages are used in patients with degenerative disc disease or spinal instability (Figure 3). PEEK cages have shown satisfactory outcomes in several clinical studies, with high interbody fusion rates and few complications being reported even with follow-up of up to 35 months (122-124). Moreover, PEEK implants are used in several other orthopedic applications, such as in total joint replacement (i.e., of the hip and knee) (105) and as fixation screws in trauma surgery (11).

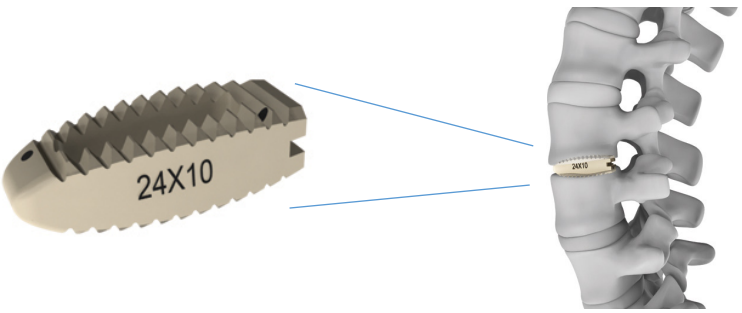

Figure 3. Image of PEEK thoracolumbar interbody cage that is used for posterior lumbar interbody fusion procedures. Images provided courtesy of GESCO Healthcare Pvt. Ltd.

PEEK is also used in dental applications and in maxillofacial surgery (125). In the field of oral prosthodontics, interest in PEEK as a material for reconstructive applications (Figures 4 and 5) has increased in the last few years, despite the fact that only a few relevant clinical studies have been reported (18). Furthermore, the possibility to manufacture constructs that contain PEEK using Computer-Aided Design / Computer-Aided Manufacturing (CAD/CAM) allows for a completely digital workflow that is both time- and cost-effective (126). Using CAD/CAM also enables additive manufacturing techniques (e.g., 3D printing), to produce devices for dental applications (127).

PEEK may be used for tooth- or implant-supported fixed dentures (i.e., bridges and crowns) (128). Provisional fixed dentures are usually made of methacrylates, such as PMMA or composite-based materials (129). However, due to their low-level mechanical strength, these restorations are not as long-lasting as the metals and ceramics used in permanent restorations. As a replacement for acrylic resins, PEEK may be suitable for long-term provisional restorations, considering that it is a "stronger" material. It has also been suggested that PEEK could be used in removable dentures, such as complete and partial dentures, as well as in removable obturator prostheses due to its low weight and favorable biocompatibility profile (130, 131). As described in the *Introduction* section, residual monomers can leak out of methacrylate-based materials into the saliva and cause allergic reactions. PEEK, being a chemically stable polymer, could therefore be used as an alternative to methacrylates such as PMMA in removable dentures.

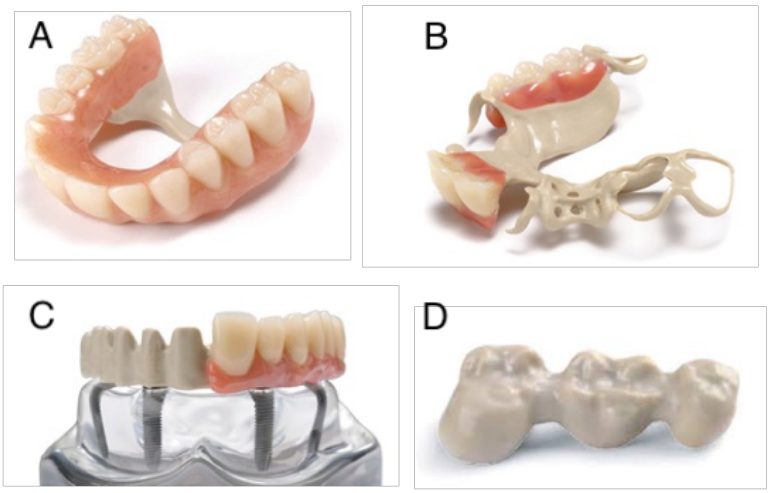

Figure 4. Prosthetic devices made from PEEK-OPTIMA™ (JUVORA™ Dental Disc): A) Removable implant-supported overdenture. B) Removable partial denture. C) Fixed implant-supported prosthesis. D) Fixed partial denture. Images provided courtesy of Invibio Biomaterial Solutions.

Even though dental osseous PEEK implants to replace missing teeth have been reported, more clinical studies are required to assure favorable outcomes (132). The biocompatibility of titanium used as an osseointegrated implant to replace missing teeth has been demonstrated in several long-term studies (133). Therefore, it is difficult to argue that PEEK might replace titanium as the material of choice for dental implants. However, PEEK may be used as a material in healing abutments and provisional implant-supported crowns (116, 134, 135). The abutments can easily be modified by the clinician for mucosal formation and support. Moreover, considering the biocompatibility of PEEK and the mechanical properties of the material, it may be suitable for use in the oral clinical setting.

Figure 5. Temporary abutment made from PEEK. Image provided courtesy of © Nobel Biocare Services AG.

2 BACKROUND TO THE PRESENT THESIS

PEEK is used in medical and dental applications due to its favorable properties of high mechanical strength, chemical resistance, and biocompatibility. However, studies related to the biocompatibility, inflammatory and biofilm formation properties of PEEK are scarce. Therefore, it is of interest and essential to increase our basic understanding of the potential of PEEK as a material that can be used in various prosthetic devices. Moreover, it is important to determine whether certain modifications to the surface of the PEEK material generate results that are of interest and that can be translated into using PEEK more broadly in prosthetic dentistry. This will increase our understanding regarding its applications and the potential risks of biological and technical complications when choosing materials for use in the clinical setting.

2.1 AIM

The overall aim of this thesis was to use in vivo and in vitro experimental methods to investigate the potential of using PEEK as a material for dental devices.

2.2 SPECIFIC AIMS

The specific aims of the studies in this thesis were:

Studies I and II: To investigate the bone tissue responses in vivo to cylinder shaped and threaded PEEK implants coated with nanoHA, as compared to uncoated PEEK implants.

Study III: To compare the early inflammatory responses in vitro to PEEK and to Ti6Al4V, and to investigate whether a rough PEEK surface influences these inflammatory responses.

Study IV: To investigate biofilm formation in vitro by applying different oral bacterial species to PEEK, blasted PEEK, cp-Ti, and Ti6Al4V.

2.3 HYPOTHESES

Studies I and II: That nanoHA-coated PEEK implants enhance osseointegration, as compared to uncoated PEEK.

Study III: That PEEK induces a stronger inflammatory response than Ti6Al4V, and that a rougher surface provokes higher levels of release of cytokines, as compared to a smoother surface.

Study IV: That bacterial adhesion and biofilm formation are affected by the composition and surface roughness of the material.

3 MATERIALS AND METHODS

3.1 MATERIALS

The following materials were used in the studies (see Section 3.3 for a description of the surface treatments). All the materials were manufactured as machined (i.e., turned).

Study I:

- **PEEK**: Polyetheretherketone
- **NanoHA-coated PEEK**: PEEK coated with nanocrystalline hydroxyapatite

Study II:

- **PEEK**
- **NanoHA-coated PEEK**

Study III:

- **PEEK**
- **Blasted PEEK:** PEEK blasted with aluminum oxide
- **Ti6Al4V:** Titanium-6 aluminum-4 vanadium ELI (Extra low interstitials)

Study IV:

- **PEEK**
- **Blasted PEEK**
- **Ti6Al4V**
- **Cp-Ti**: Commercially pure titanium grade 4

3.2 IMPLANT MANUFACTURING

In **Study I**, cylinder shaped PEEK implants were used. In **Study II**, the implants were threaded. In the in vitro studies (**Studies III** and **IV**), the materials were manufactured as coin-shaped disks. The designs of the different implants/materials are shown in Figure 6.

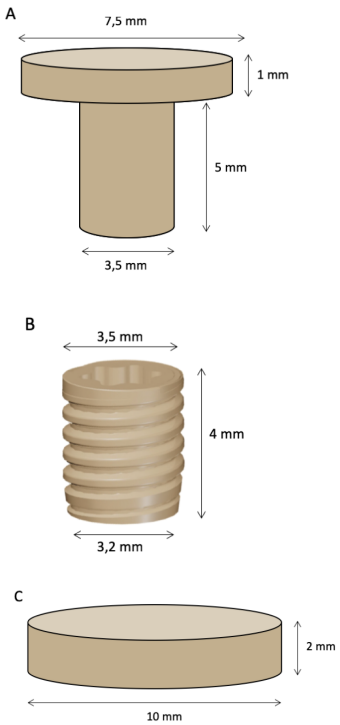

Figure 6. Geometries of the samples used in:
(A) Study I; (B) Study II; and (C) Studies III and IV.

Sample cleaning and sterilization
The samples in **Studies III** and **IV** were ultrasonically cleaned once with 1% Extran® AP15 (Merck, Darmstadt, Germany) in 60°C tapwater for 15 minutes. Thereafter, the samples were rinsed in distilled water and immersed in 70% ethanol for 15 minutes.

The implants and samples in **Studies I**, **III** and **IV** were packed in sterilization pouches, which were sealed and sterilized in an autoclave (Getinge AB, Getinge, Sweden) at 134°C and 3 bar using a 60-minute sterilization program.

The implants used in **Study II** were disinfected by immersion in a 70% ethanol solution and then dried at 120°C.

3.3 SURFACE TREATMENTS

NanoHA coating
The surfaces of the test implants used in the in vivo studies (**Studies I** and **II**) were modified with nanocrystalline hydroxyapatite (nanoHA), provided as HA^{nano} Surface (Promimic, Mölndal, Sweden). The coating procedure is described in detail in the patent description (136). Briefly, nanoHA particles made of synthetic crystalline calcium phosphate (average particle size range, 1–10 nm) are dissolved in a solution. The liquid is applied to the implant surface by spin coating, whereby the implant is rotated at 2,700 rpm for 5 seconds. This results in an evenly dispersed coating, giving an approximately 5–20 nm-thin layer of crystalline nanoHA.

Aluminum oxide blasting
One group of the PEEK samples used in the in vitro studies (**Studies III** and **IV**) was surface-treated with abrasive blasting using 110-µm aluminum oxide particles (Al_2O_3) at an air pressure of 2 bar.

3.4 SURFACE CHARACTERIZATIONS

Scanning electron microscopy
The surfaces of the materials were examined in all four studies with scanning electron microscopy (SEM). Images of the surfaces were used to describe visually the surface characteristics of the implants and coins. Surfaces that were cultured with PBMCs (**Study III**) and bacteria (**Study IV**) were also imaged. The samples were coated by sputtering with gold or palladium, in order to eliminate any charge effect and improve the contrast of the image. The

images were acquired at various magnifications (200× up to 60,000×), with different brands of microscopes being employed in the various studies (**I–IV**).

The following types of SEM equipment were used in the studies:
- **Studies I** and **II**: LEO Ultra 55 FEG (Carl Zeiss, Oberkochen, Germany).
- **Study III**: Carl Zeiss DSM 982 Gemini (Carl Zeiss).
- **Study IV**: Zeiss Evo MA10 (Carl Zeiss).

Chemical surface compositions
The elemental compositions of the sample surfaces were analyzed in **Study I** with x-ray photoelectron spectroscopy (XPS) (PHI 5500 ESCA system; Perkin Elmer, Wellesley, MA, USA) and in **Study IV** using energy-dispersive an x-ray spectroscope (EDX) and LEO Ultra 55 SEM (Carl Zeiss), equipped with an EDX detector (Inca, Oxford, UK).

Optical interferometry
Surface roughness at the micrometer level was determined in the four studies using an optical interferometer together with an image analysis program. In **Study II**, the measurements were performed at the threaded tops.

The following interferometers were used in the studies:
- **Studies I** and **II**: MicroXam (ADE Phase Shift Inc., Tucson, AZ, USA) evaluated with the SurfaScan software (Somicronic Instrument, Lyon, France).
- **Study III**: MicroXAM 100-HR (ADE Phase Shift Inc., Tucson, AZ, USA) evaluated with the MountainsMAP Premium ver. 7 software (Digital Surf, Besançon, France).
- **Study IV**: SmartWLI-extended (GBS mbH, Ilmenau, Germany) and the SmartVIS3D software ver. 2.1 (GBS), with processing using the MountainMaps software version 7.4 (Digital Surf).

The following parameters were measured:
1. Sa (μm) = average roughness; average height deviation from a mean plane within the measured area.
2. Sds ($1/\mu m^2$) = summit density; the number of summits per unit area.
3. Sdr (%) = developed interfacial area ratio; the additional surface area contributed by the roughness, as compared with a totally flat plane.
4. Sci = core fluid retention index (only in **Study I**).

The definitions of surface roughness were according to Albrektsson and Wennerberg (137):
- Smooth surface: Sa value of <0.5 μm.
- Minimal rough surface: Sa value of 0.5–1.0 μm.
- Moderately rough surface: Sa value of 1–2 μm.
- Rough surface: Sa value of <2 μm.

Atomic force microscopy (Study I)
Topographic analysis on a nanometer level was performed with an atomic force microscope (Digital Instruments, Santa Barbara, CA, USA). The following parameters were measured: Sa (nm), Sds, and Sdr. The measurements were further analyzed to determine the grain diameter and the mean height.

Contact angle measurements (Studies III and IV)
The wettability of the samples was analyzed by measuring the water contact angles (θ). This is a simple method to measure the surface free energy of a material. Sessile droplets of water were applied to the samples and the angle between the liquid and the surface was measured. A surface is defined as more hydrophobic the larger the contact angle.

The following instruments were used to measure the water contact angles:
- **Study III**: DSA100 goniometer (Krüss GmbH, Hamburg, Germany).
- **Study IV**: JVC-3CCD video camera (JVC, Yokohama, Japan) with the Optimas ver. 6.5 image analysis software (Optimas Inc., Glenview, IL, USA).

3.5 SURGICAL TECHNIQUES AND IMPLANT INSERTION

The in vivo studies (**Studies I** and **II**) involved 9 and 13 mature New Zealand White female rabbits, respectively.

Antibiotics were administered prophylactically at the time of surgery and for 3 days post-surgery (specific doses, medications and suppliers are listed in the articles). The animals were kept in separate cages and had free access to tapwater and a standard diet, according to the in-house standard at the animal facility.

For the surgery, the animals were anesthetized with intramuscular injections of fentanyl and fluanisone and an intraperitoneal injection of diazepam. Local anesthetic of lidocaine was injected at the site of implant insertion and the hind

legs were shaved and cleaned. Incisions of the skin and facial layers were made, and the periosteum was gently pulled away to expose the bone surface and was not re-sutured. The implant sites were prepared using a low-speed bur with a graded series of drills of increasing diameter under saline irrigation and aseptic conditions. Tapping was performed before the implants were seated (**Study II)**. After the surgery, the fascia and the skin were sutured separately. The same person inserted all implants. In **Study I**, the cylindrical part of the implant was placed in the bone tissue with the cap on top of the cortical bone. In **Study II**, the implants were placed in the bone so that the uppermost thread was at the same level as the cortical surface, so as to optimize the primary stability. No complications were noted for the animals during the follow-up period. Six weeks after surgery, the animals were first sedated and then sacrificed.

The studies consisted of the following experimental groups:

Study I: In total, 18 implants were used. One test implant (n=9) and one control (n=9) implant were inserted in each femoral metaphysis in the condyle region in the same animal.

Study II: A total of 78 implants was used in the study. Each animal received six implants: one was inserted in each femur metaphysis in the condyle region (test in one leg and control in the other leg) and two were inserted in each tuberositas tibia region (test implants in one leg and controls in the other, with approximately 5 mm between the proximal and distal implants) (Figure 7).

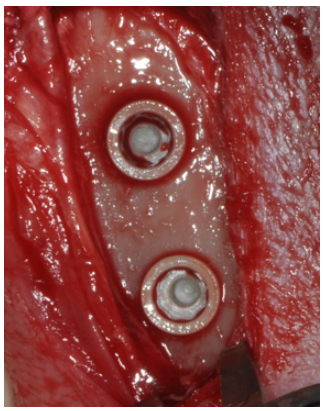

Figure 7. Image taken during surgery after the insertion of two screw-shaped PEEK implants in the proximal (upper) and distal (lower) areas of the tibial bone. The outer diameter of the implant is 3.5 mm.

3.6 ETHICAL CONSIDERATIONS

The studies were approved by the local Animal Ethics Committee at Gothenburg University and the studies were conducted in accordance with the specific rules of ethics.

3.7 HISTOLOGIC METHOD AND ANALYSES

Tissue preparation
The femur implants (**Studies I** and **II**) were removed *en bloc* with the implant *in situ* and further processed in the laboratory according to the in-house standard technique, resulting in undelacified cut and ground sections, as described by Donath (138).

In brief, the sample processing involved: immersion fixation in 4% neutral buffered formaldehyde, rinsing in tap water, dehydration in an ethanol series (70% to absolute ethanol), pre-infiltration in diluted resins, and finally embedded in pure resin (Technovit 7200 VLC; Heraeus Kultzer GmbH, Wehrheim, Germany), followed by light-curing.

The preparation of undecalcified cut and ground sections, with implants *in situ*, was performed with the so-called Donath technique, using the EXAKT cutting and grinding equipments (EXAKT Apparatebau GmbH, Norderstedt, Germany). The cured samples were divided in the longitudinal direction of the implant, in a water-cooled bandsaw. In order to obtain a plane parallel sample surface, the divided bloc was ground with SiC wet grinding paper (800–1200 grit size) in the water-cooled grinder.

A supporting plexi-glass was glued onto the sample and at least one section with a thickness of about 200 µm was cut and ground to a final thickness of about 15 µm (139). All the sections were histologically stained with toluidine blue mixed with pyronin G, and the most central section of each implant was used for the quantitative analysis (140).

Study I:
The quantitative measurements were performed using a light microscope (Eclipse ME 600L; Nikon, Tokyo, Japan) and an image analysis program (Image Analysis 2000; Tekno Optik AB, Huddinge, Sweden). Both the 4× and 10× objectives were used, rendering 40× and 100× magnifications, respectively, in the microscope. All measurements were performed directly on the screen by the same person.

- The percentage of bone-to-implant contact (BIC) was quantified along the implant surface on each side of the implant, and a mean value was calculated.

- Bone area (BA) was measured in four similar-sized regions of interest (ROI) (Figure 8). The mean values were calculated for: i) the upper region parts (1 and 3); and ii) the lower parts of the sample (2 and 4).

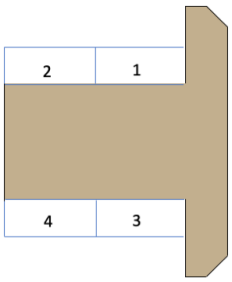

Figure 8. Cross-section of the PEEK implant, used in Study 1, showing the regions of interest around the implant in which measurements of the bone-to-implant contact (measured at the interface on each side of the implant and presented as the mean value) and the bone area (measured in each of the four boxes and presented as the mean value) were performed.

Study II:

- The percentage BIC was quantified using the Leitz Metallux 3 light microscope (Leitz GmbH, Wetzlar, Germany) coupled to a Leitz Microvid unit connected to a PC. The measurements were performed directly in the eyepiece of the light microscope using the 10× and 16× objectives, rendering magnifications of 100× and 160×, respectively. Measurements of the percentage BIC were performed along the entire length, on both sides of the implant, e.g., in each thread and in between the threads. All the measurements were performed by the same person.

- For bone area (BA) measurements, microscopic images were acquired with the Nikon DS-Ri1 camera connected to a light microscope (Eclipse ME 600L; Nikon) with a 5× objective. These images were used to quantify the BA with a semi-automatic image analysis software, i.e., Cuanto Implant (Uppsala, Sweden) (141). The BA percentages were calculated in all threads on both sides of the implant. The calculations were made for the following regions of the implant (Figure 9):

(i) in all threads around the entire implant;
(ii) in the three best consecutive threads; and
(iii) in the three best 'mirror image (MI) BAs' outside the three best consecutive inner threads (142). All measurements were performed by the same person.

In addition to the histomorphometric quantification, a qualitative histologic inspection and description of the tissue close to the implant were performed. Objectives up to 50× were used.

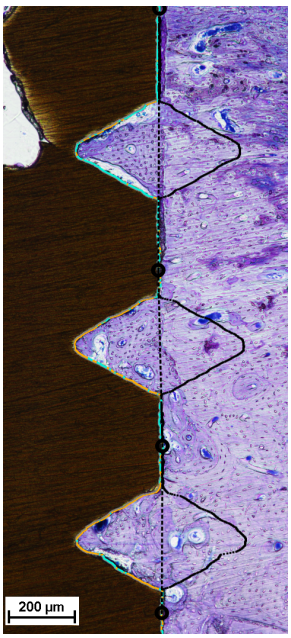

Figure 9. Histologic stained cut and ground section of a PEEK implant in femur demonstrating the semi-automatic measurements of bone area (BA) both inside the threads and in the mirror image (MI) region outside the same threads. Scale bar: 200 µm.

3.8 BIOMECHANICAL TESTS

Thirty-two of the implants in the tibia (**Study II**) were investigated with the removal torque (RTQ) test, which was performed with a manual torque wrench with a strain gauge (BTG90CN-S; Tohnichi, Tokyo, Japan). In three rabbits, both tibial implants were removal torque-tested (n=12), while the distal implants in ten rabbits were tested (n=20). The proximal implants in these rabbits were retrieved for further analysis (results not reported in this study).

The RTQ test itself is a destructive shear strength test that provides a direct reading of the level of torque (in Newton centimeters; Ncm) that is required to loosen the implant from the bone bed.

3.9 CYTOKINE AND CELL ANALYSES

Isolation and culturing of human blood cells
In **Study III**, peripheral blood mononuclear cells (PBMCs) were isolated from the buffy coats of 10 healthy blood donors. The PBMCs were extracted by centrifugation of the buffy coat over a density gradient, so as to separate the buffy coat into layers depending on the density of the different cell types. The intermediate layer containing the PBMCs was collected and the PBMCs were cultured in the presence of the different materials to be tested in 24-well polystyrene plates. The polystyrene well served as a control surface. Culture supernatants were collected after 1, 3, and 6 days of incubation for cytokine analysis.

Cytokine assay
For quantification of the cytokines in the culture supernatants, the Bio-Plex Pro Human Cytokine Assay (Bio-Rad Laboratories, Hemel Hempstead, UK) was used. This assay allows multiple cytokines in one sample to be quantified simultaneously. The samples were incubated with sets of distinctly color-coded beads that were conjugated with capture antibodies directed against a desired biomarker (e.g., a cytokine). A detection antibody was added and allowed to react with the bound proteins of interest. Finally, streptavidin-conjugated phycoerythrin was added to create the final detection complex (Figure 10).

The data were acquired using the BioPlex 200 instrument equipped with the accompanying software (Bio-Rad Laboratories). The different colors on the beads were detected with a laser so as to distinguish the color codes, i.e. each analyte-specific set of beads, from each other. The cytokine concentrations were calculated by comparing the mean fluorescence intensity for each set of

beads against an automatically optimized and manually verified standard curve. The Hierarchical Clustering Explorer ver. 3.0 software (University of Maryland, USA; www.cs.umd.edu/hcil/hce/hce3.html) was used to create a heat map that visualized the patterns of expression of the selected cytokines.

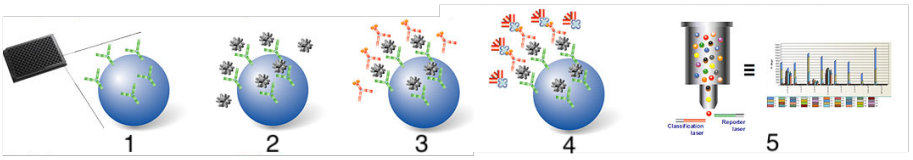

Figure 10. Schematic protocol of the Multiplex Immunoassay: 1. Color-coded beads coated with analyte-specific capture antibodies. 2. The antibodies bind to the desired biomarker (e.g, a cytokine). 3. Biotinylated detection antibodies bind to the analytes of interest and form an antibody-antigen sandwich. 4.Phycoerythrin (PE)-conjugated streptavidin binds to the biotinylated detection antibodies. 5. The fluorescence intensity is detected with laser and the data is analyzed. Image provided courtesy of Bio-Rad Laboratories, Inc.

Fixation of cells

Samples from the 3-day cultures of PBMCs were selected for fixation of the cells to the material surface. These samples were used to visualize the attached cells using SEM.

The PBMCs attached to the surfaces of the materials were also quantified using immunofluorescence. The cells attached to the coins were fixed by direct transfer of the coins into 4% paraformaldehyde (PFA). After 25 minutes, washing with Tris-buffered saline (TBS) was performed to remove the PFA, as well as any unattached or loosely attached cells.

The coins were mounted using the ProLong antifade reagent and the cells were stained with 4′6-diamidino-2-phenylindole (DAPI) (Molecular Probes, Eugene, OR, USA). DAPI is a blue fluorescent stain that binds to DNA and reveals all nucleated cells. Microscopy was performed using an inverted LSM 700 confocal microscope (Carl Zeiss Microscopy GmbH, Jena, Germany) and the images were captured using a Plan-Apochromat 40×/1.3 oil objective. To obtain representative data, images were acquired at nine standardized locations starting at the center of each coin with 1 mm in the x and y distances between

the sites. The quantification of adherent cells was performed both manually and automatically using a cell counter software.

Analysis of Z-stack images
Z-stack sampling was obtained to create a three-dimensional representation of the cells located on the surface. This was performed with the confocal microscope together with the ZEN image software (Carl Zeiss Microscopy). Apart from staining nucleated cells with DAPI (blue), CD14 (green) and integrin CD11b (red) were also stained. Unspecific binding was blocked using 1% normal goat serum, 1% donkey serum and 1% Bovine serum albumin (BSA) (Sigma-Aldrich, St. Louis, MO, USA) in TBS after which the primary antibodies, rabbit anti-CD11b (clone EPR1344; Abcam, Cambridge, UK) and mouse anti-CD14 (clone 2Q1233; Abcam), were added and allowed to bind overnight. Antigen-specific binding was visualized using Alexa Fluor 488-conjugated goat anti-mouse IgG and Alexa Fluor 647-conjugated donkey anti-rabbit IgG (both from Abcam).

3.10 MICROBIOLOGICAL PROCEDURES

In **Study IV**, the following four bacterial species were cultured separately on the materials to be tested: *Streptococcus sanguinis* (ATCC 10556), *Streptococcus oralis* (ATCC 35037), *Enterococcus faecalis* (ATCC 19433), and *Streptococcus gordonii* (ATCC 10558). All the bacteria were cultured on tryptone soya agar and incubated at 37°C for 24–48 hours to obtain single colonies. A single colony was suspended in a growth medium that contained sucrose. For comparison, *S. gordonii* was also cultured in the growth medium in the absence of 1% sucrose. *S. sanguinis, S. oralis* and *E. faecalis* were cultured with the sample materials for 72 hours and 120 hours, while *S. gordonii* was cultured with the sample materials for 48 hours.

Biofilm Assay
Biofilm formation was quantified using a modification of the method of Christensen et al. (143). Briefly, fixation of the biofilm was carried out by immersing the samples in 10% formalin. Crystal violet stain was added for 5 minutes and then rinsed to remove excess stain. After drying, the crystal violet was solubilized by immersion in methanol. The samples were removed and the absorbance at 590 nm was read in a spectrophotometer (Jenway model 7315; Jenway Ltd., Stone, Staffordshire, UK). The absorbance of the eluted stain was proportional to the concentration of bacteria present on the sample surface.

3.11 STATISTICAL ANALYSES

The following statistical methods were used in the studies:

Study I The interferometry and the histomorphometric analysis were performed using the Mann-Whitney U-test.

Study II The histomorphometric data and the RTQ test results were analyzed with the Wilcoxon signed-rank test.

Study III The interferometry was tested by one-way ANOVA followed by Tukey's post-hoc test. The results of the Bio-Plex assay and the immunofluorescence images were analyzed with the Wilcoxon matched-pairs, signed-rank test.

Study IV The results of the interferometry, contact angle, and biofilm measurements were analyzed by one-way ANOVA followed by Tukey's post-hoc test. Two-way ANOVA followed by Tukey's post-hoc test was used to compare the effect of the two independent variables (i.e., material and time) on biofilm formation.

Statistical significance in all studies was evaluated using the SPSS ver. 21.0 software (SPSS IBM, Chicago, IL, USA). The results from the Bio-Plex assay and the immunofluorescence images in **Study III** were processed using the GraphPad Prism ver. 7.0 software (GraphPad Software Inc., La Jolla, CA, USA). The contact angle measurements in **Study IV** was evaluated with Minitab 17 statistical software (Minitab Inc. State College, PA, USA).

4 RESULTS

4.1 SURFACE CHARACTERIZATIONS

Scanning electron microscopy
The SEM examination of the implant surfaces revealed the presence of nanoHA crystals on the coated test implants (**Studies I** and **II**) (Figure 11).

The SEM of the blasted PEEK material clearly showed abrasive pits, due to blasting the PEEK surface with aluminum oxide (**Studies III** and **IV**). Images of the PBMCs cultured on the samples (**Study III**) showed that the rougher the surface the more numerous were the attached cells (Sa values: blasted PEEK >PEEK >Ti6Al4V) (Figure 12).

The same trend was seen for biofilm formation, where the numbers of bacteria were higher on the rougher surface (**Study IV**) (Figure 13).

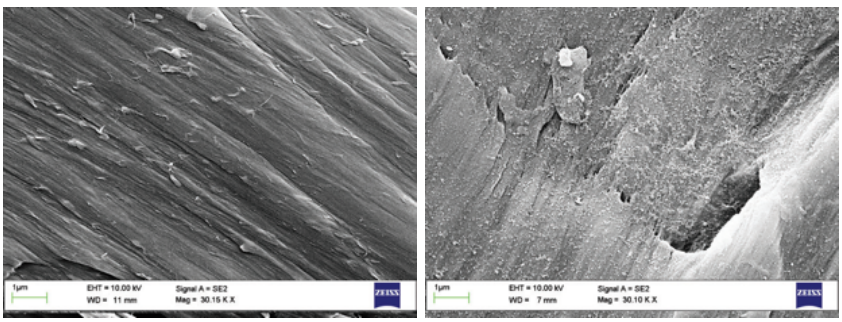

Figure 11. SEM images of untreated PEEK (left) and nanoHA-coated PEEK (right) surfaces at ×30,000 magnification. Scale bar: 1 µm.

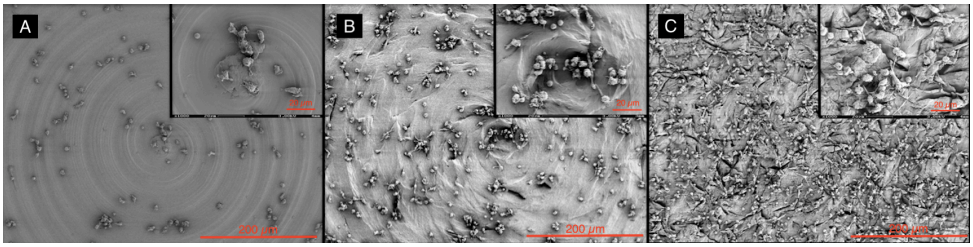

Figure 12. SEM images of Ti6Al4V (A) PEEK (B), and blasted PEEK (C) after 3 days of culturing with PBMCs on the surfaces of the coins (magnification, ×200). The cells in (A) and (B) are sparsely dispersed in groups of cells that align with the spiral texture of the surface, while on the blasted surface (C), the cells are more frequently distributed and almost "captured" in the pits of the surface. Bar: 200 µm. A zoomed image (magnification, ×1000) is shown in the upper-right corner. Bar: 20 µm.

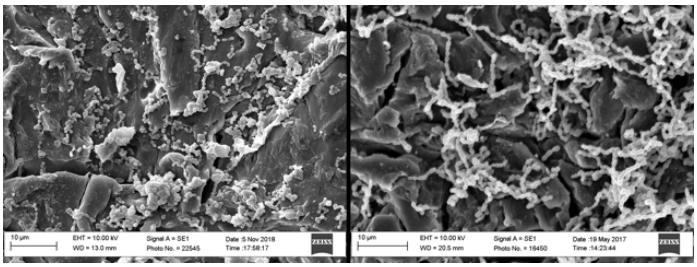

Figure 13. S. oralis (left) and S. gordonii (right) biofilms on blasted PEEK after 48 hours of culturing. Some chains of bacteria (light appearing structures) can be seen lying within the cracks and crevasses. Bar: 10 µm.

Chemical surface compositions

The results of the chemical analyses confirmed the material compositions of the surfaces.

Study I: The XPS analysis on the nanoHA-coated implants revealed that the calcium and phosphate concentrations were 8.7 and 5.2 atomic%, respectively, corresponding to a Ca/P ratio of 1.67, which is the stoichiometric ratio of HA.

Study IV: The results from the EDX analysis confirmed the expected purity of cp-Ti and the composition of Ti6Al4V. Small amounts of Al were detected in the blasted PEEK samples, most likely due to remnants of the Al_2O_3 blasting media being lodged in the surface.

Optical interferometry

The test implants used in **Study I** showed smooth surfaces on the micrometer level (Sa < 0.5 µm), while the control implants had minimally rough surfaces (Sa = 0.5-1.0 µm), as defined by Albrektsson and Wennerberg (137). Both the test and control implants in **Study II** also showed minimally rough surfaces. In **Study I**, the nanoHA-coated implants had smoother surfaces according to the parameters Sa, Sds and Sdr, as compared to the control implants. In **Study II**, small differences were noted between the control and test implants with respect to all the parameters tested (Sa, Sds, and Sdr). The microstructure of the surface of the blasted PEEK was rougher and yielded higher mean values for all the parameters, as compared to the other groups (**Studies III** and **IV**). The surfaces of both the cp-Ti and Ti6Al4V were significantly smoother than the PEEK surfaces. See table 2 for the Sa-values from the various studies.

Material / Sa-value µm	Study I	Study II	Study III	Study IV
PEEK	0.96 (0.28)	0.85 (0.29)	0.44 (0.10)	0.57 (0.08)
NanoHA-coated PEEK	0.41 (0.14)	0.93 (0.25)	-	-
Blasted PEEK	-	-	1.12 (0.14)	1.85 (0.19)
cp-Ti	-	-	-	0.23 (0.01)
Ti6Al4V	-	-	0.24 (0.03)	0.28 (0.01)

Table 2. Mean Sa values (µm) (SD= standard deviation) for surface topography in the various studies.

Atomic force microscopy (Study I)

The results of the AFM measurements indicated similar nano-roughness values for both the test (nanoHA) and control samples, in terms of both height deviation (Sa nm) and developed surface area ratio (Sdr %). However, the Sds (μm^{-2}) value indicated that the test surface had more densely peaked summits than the control surface, reflecting the surface modification.

Contact angle measurements (Studies III and IV)
The blasted PEEK showed the highest mean contact angle between the liquid and solid, indicating that this material was more hydrophobic than the other materials. In **Study IV**, the PEEK sample was significantly more hydrophobic than the titanium samples, although there was no statistical difference between cp-Ti and Ti6Al4V in this respect.

Surfaces after sterilization
The surface examinations (i.e., with SEM and XPS) were performed both before and after sterilization. The XPS analysis revealed that there was nanoHA present on the implant surface but in some parts of the surface the coating was undetectable. This observation lead to a change in the sterilization procedure, thus in **Study II** the implants were sterilized with 70% ethanol, rinsed in NaCl and dried.

4.2 HISTOMORPHOMETRIC ANALYSES

Study I
The implants were investigated after 6 weeks of follow-up. During harvesting of the samples, the implants were inspected grossly, i.e., to determine whether the implants were anchored in the bone or loose. Seven implants (three test implants and four control implants) failed to integrate into the bone tissue and were surrounded by soft tissue. The failed implants were excluded from the histomorphometric evaluations. Two of these implants (one test and one control) failed to integrate within the same animal. In total, 11 implants (6 test implants and 5 controls) were analyzed by histomorphometry.

The histomorphometric results showed that the nanoHA-coated implants resulted in higher mean values for BIC and BA compared to the non-coated controls, although the differences were not statistically significant (Figure 14).

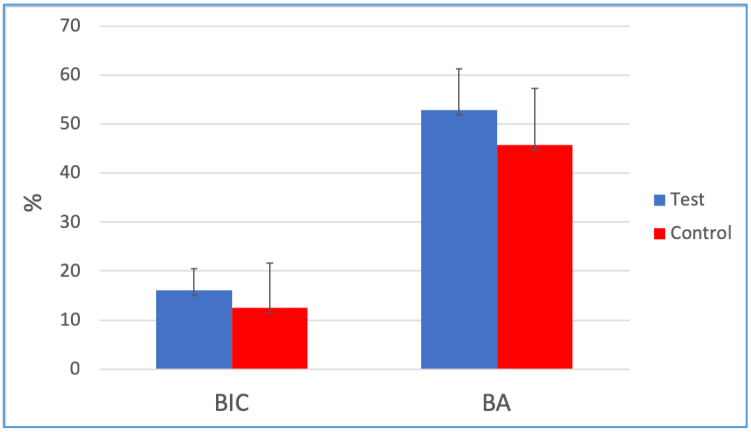

Figure 14. Bar graph showing the percentages of bone-to-implant contact (BIC) and bone area (BA) in the nanoHA-coated test implants (blue) and the uncoated control implants (red). The bars represent the mean values and standard deviation. None of the differences are statistically significant.

Study II

The animals completed the study and the gross examination revealed no loosened implants after 6 weeks of follow-up. The quantitative results (13 test implants and 13 control implants) for BIC, BA, and MI-BA (mean and standard deviation) are shown in Table 3. In general, the results of the histomorphometric evaluations for BIC (manual measurements) and BA (semi-automatic measurements) indicated higher mean values for the nanoHA-coated test implants, as compared to the control implants.

Parameter, % (SD)	Test implants	Control implants	*p*-value
BIC	39 (14)	33 (12)	0.02
BA, all threads	68 (12)	68 (9)	n.s.
BA, three best	90 (3)	87 (4)	0.05
MI BA, three best	96 (2)	98 (1)	n.s.

n.s., Not significant. Test implants = NanoHA coated PEEK. Control implants = uncoated PEEK.

Table 3. Mean values for the percentages of bone-to-implant contact (BIC) along the length on both sides of the implant. The bone area (BA) values are presented for all the threads and the three best consecutive threads. Mirror image bone areas (MI BA) are presented for the three best consecutive outer threads. The standard deviation is given within the parentheses. The results were analyzed with the Wilcoxon signed rank-test with significance level set at $p \leq 0.05$.

4.2.1 Qualitative histologic observations

The most striking qualitative observation (**Study II**) of both the test and control samples involved the numerous bone-forming regions in close vicinity to the implants, although osteoblasts were difficult to detect on the osteoid. Moreover, elongated and stretched-out FBGCs/MNGCs, appearing like a two-cell layer collar close to the implant surface was observed. Some, possibly detached, implant fragments could also be observed in the phagocytic cells. Further histological description in Figure 15.

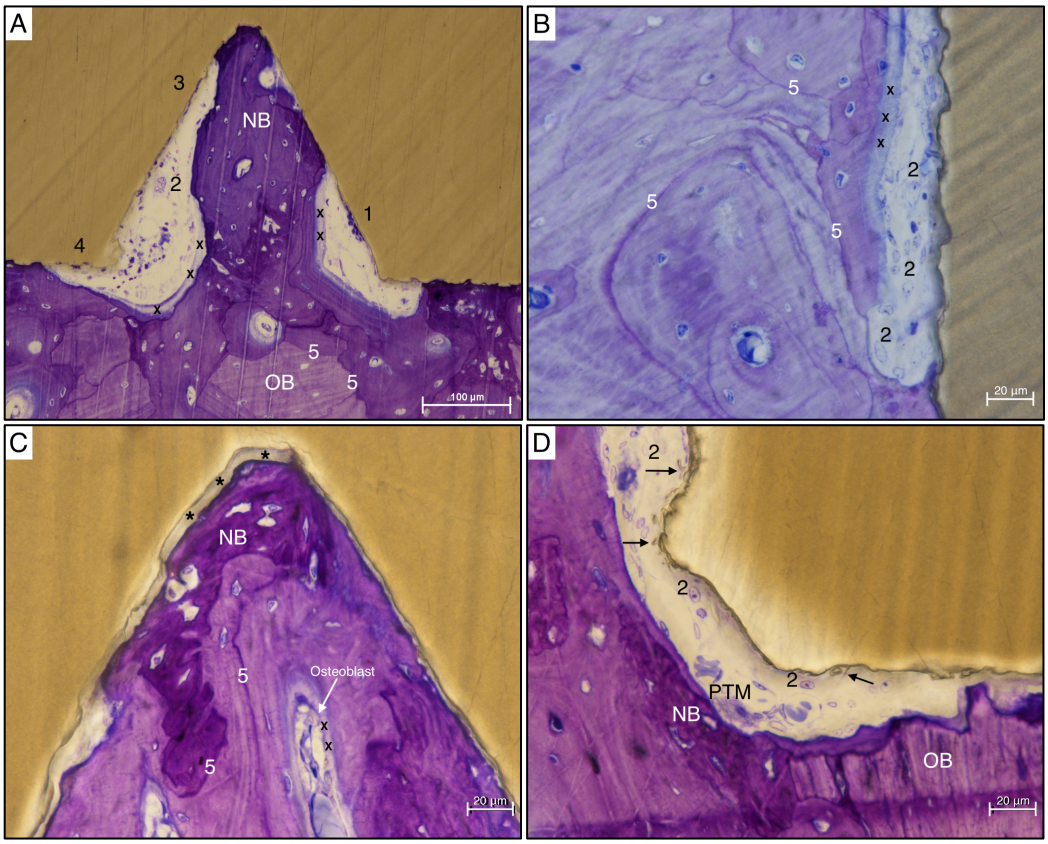

Figure 15.

A) Test nanoHA-coated PEEK implant, demonstrating newly formed bone (NB) (dark purple) inside the threaded region of the implant. Bone-forming surfaces, i.e., osteoid rims (greyish appearance) can be seen, albeit in the absence of osteoblasts (x). The soft-tissue regions that separate the implant and the bone contain light- and darker-stained cells, the majority of which are macrophages of various sizes. Close to the implant interface surface (right-hand side), a rim of darker-stained oval cells is visible. This structure is most likely an elongated foreign body giant cell (1). Large light appearing macrophages are visible in the soft-tissue area. The soft-tissue region on the left-hand side contains mostly macrophages (2). In the middle part of this soft-tissue region one can observe a large light formation with cells that resemble large macrophages, which are internalized in this structure. A thin rim of darkly stained cells and single cells can be observed in the interface region (3). Note the irregular thread surface (left side), which is seemingly a trap for (darkly stained) macrophages (4). Lighter-stained old bone (OB) is clearly separated from the new bone by cement-lines (5). Scale bar: 100 µm.

B) Test nanoHA-coated PEEK implant. Mostly newly formed bone is present in this section. An osteoid rim (greyish structure), seemingly devoid of osteoblasts, is visible on the bone surface (x). A soft-tissue region, containing macrophages of various sizes and shapes, separates the bone from the irregularly shaped implant surface. The large macrophages may represent the so-called "frustrated" macrophage types (2). Some of the "loosely packed macrophages" appear as "phagocyte-type" macrophages (having an irregular surface and vesicles in the cytoplasm). Cement-lines separate the various maturation forms of the bone (5). Scale bar: 20 µm.

C) Control uncoated PEEK implant, demonstrating mostly newly formed immature bone (dark purple) in the thread (NB). The PEEK surface appears to be smooth, and there is a shrinkage artifact between the implant and the tissue (asterisks). This artifact is most likely due to fixation. Bone formation is ongoing and is clearly apparent in the center of the bone, together with osteoblasts on the osteoid rim (x). Cement-lines are visible as demarcation lines between the different stages of ongoing bone maturation (5). Scale bar: 20 µm.

D) Control uncoated PEEK implant, showing a "smoother" surface than the nanoHA-blasted PEEK surface (Figure 15 A and B). Macrophages (2) and a few plasma cells are visible in the soft-tissue region that separates the implant from the bone tissue. A rougher implant surface is visible (upper-left side) where cells are detected in the interface region. Some small, loose implant-material fragments are located outside the implant surface (arrows). The large cells located close to the bone (lower left side) are considered to be "phagocyte-type" macrophages (PTM), based on their size and the presence of vesicles in the cytoplasm. Scale bar: 20 µm.

4.3 BIOMECHANICAL TESTS

The RTQ tests in **Study II** showed a statistically significant higher mean value for the nanoHA-coated PEEK implants (15.4 Ncm), as compared to the uncoated PEEK implants (8.5 Ncm), $p = 0.001$.

4.4 CYTOKINE AND CELL ANALYSES

The results obtained from the multiplex cytokine array in **Study III** were incorporated into a heat map, in order to visualize the patterns of expression of the cytokines. The heat map represents the median concentrations of the cytokines present in the supernatants of the cultures of PBMCs exposed to the various materials.

The expression levels of the pro-inflammatory cytokines IL-1β, IL-4, IL-6, TNF-α, IFN-γ and IL-17 were selected for statistical analyses. After 3 days of culturing, the concentrations of these cytokines were significantly higher in the supernatants of PBMC cultures that contained PEEK, as compared to PBMC cultures that contained Ti6Al4V (Figure 16). With the exception of IL-17, the levels of the selected cytokines induced by exposure to the blasted PEEK were significantly higher than those induced by the machined PEEK.

In general, Ti6Al4V tended to induce lower levels of pro-inflammatory mediators than the two PEEK materials. For the majority of the cytokines, their concentrations increased when the cells were cultured in the presence of blasted PEEK, as compared to culturing with machined PEEK.

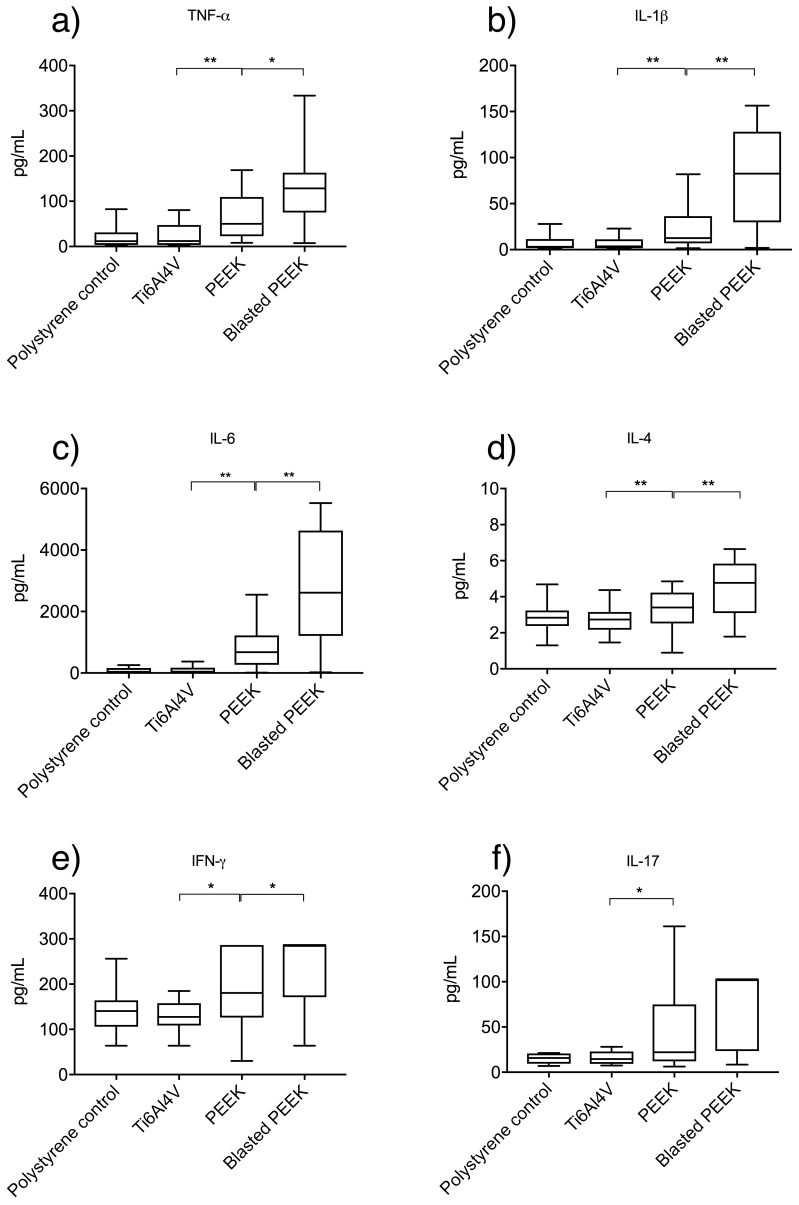

*Figure 16. Cytokine production by PBMCs exposed to Ti6Al4V, PEEK, and blasted PEEK or to a polystyrene control surface. The concentrations (pg/mL) of (a) TNF-α, (b) IL-1β, (c) IL-6, (d) IL-4, (e) IFN-γ, and (f) IL-17 were measured in the supernatants of PBMCs that were cultured for 3 days. Significant differences in concentrations comparing Ti6Al4V with PEEK and PEEK with blasted PEEK are assessed using the Wilcoxon matched-pairs signed-rank test, and denoted as follows: *, $p<0.05$; and **, $p<0.01$.*

Immunofluorescence measurements

The PBMCs attached to the material surfaces were examined using immunofluorescence confocal microscopy. The results of the manual and automatically generated measurements were compiled to derive the mean values. Significantly higher numbers of PBMCs adhered to the PEEK surfaces than to the Ti6Al4V surface (Figure 17). However, the numbers of PBMCs that adhered to the blasted PEEK surface were not significantly higher than those that attached to the machined PEEK ($p = 0.16$).

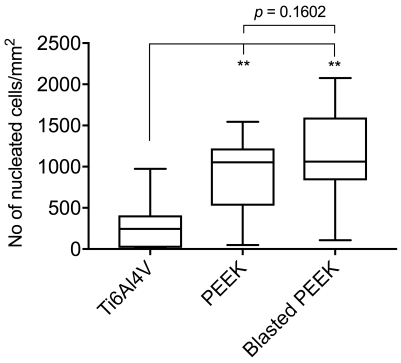

*Figure 17. Graph showing the numbers of PBMCs adhering to the coins after 3 days in culture. The results are presented as cell number per mm². **, p<0.01.*

Analysis of Z-stack images

Immunofluorescent confocal z-stack images of the PBMCs attached to the different materials are shown in the orthogonal view mode in Figure 18.

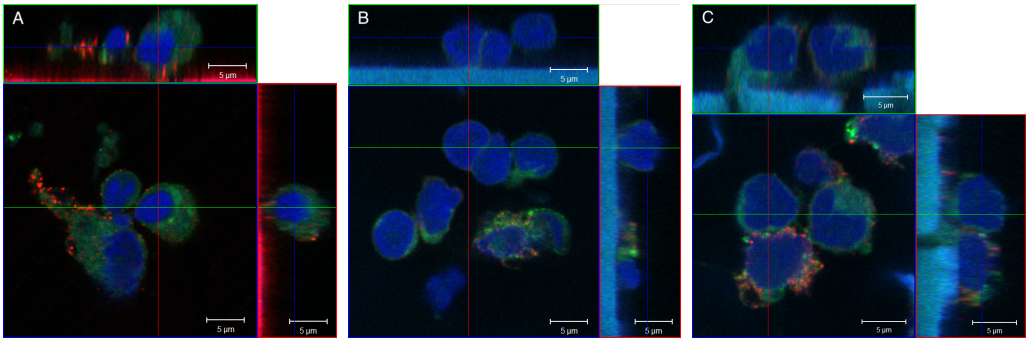

Figure 18. Z-stack confocal microscopy images of PBMCs adherent to: A) Ti6Al4V; B) PEEK; C) blasted PEEK. It seems that the cells in figure C are larger compared to the cells in figure A and B. Scale bar: 5 µm.

4.5 BIOFILM FORMATION

The results of the biofilm culturing followed by crystal violet staining (**Study IV**) showed significantly higher absorbance (590 nm) for *S. sanguinis* binding to PEEK and blasted PEEK, as compared with adherence of these bacteria to Ti6Al4V. *S. oralis* formed significantly more biofilm on the blasted PEEK compared to the other materials, whereas biofilm formation by *E. faecalis* was significantly greater on cp-Ti than on the other three materials. *S. gordonii* biofilm formation was more extensive on blasted PEEK than on PEEK (Figure 19).

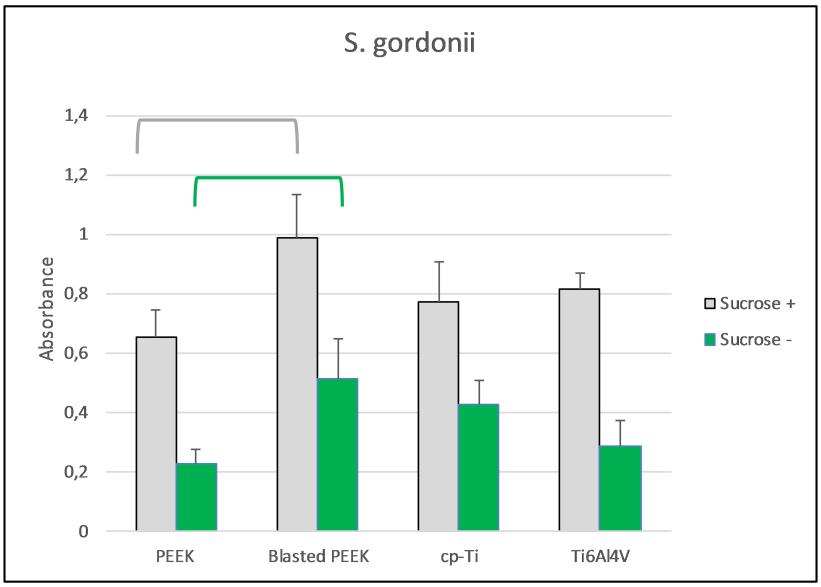

Figure 19. Biofilm formation of S. gordonii at 48 h. The bar graph shows crystal violet 590 nm mean absorbance and standard deviation, in the presence (grey) and absence of 1% sucrose (green). A significant difference was observed between PEEK and Blasted PEEK (demonstrated with brackets) in both sucrose conditions. There was no significance difference in the amount of biofilm formation on cp-Ti and Ti6Al4V compared to the other groups. Tested with One-Way ANOVA $p<0.05$ followed by Tukey's post-hoc test.

5 DISCUSSION

5.1 STUDIES I AND II

The overall objectives of **Studies I** and **II** were similar: to compare the bone responses to PEEK implants coated with nanoHA and uncoated implants. However, in **Study I**, the implants were cylinder shaped, whereas in **Study II** the implants were threaded.

In **Study I**, the cylinder shaped nanoHA-coated implants in the rabbit tibias had a higher percentage BIC 6 weeks post-surgery. However, the differences were not statistically significant. The results from **Study II** show that the nanoHA-coated, threaded PEEK implants demonstrated a higher degree of osseointegration than the uncoated threaded implants, after 6 weeks of healing. These results were confirmed by significantly higher removal torque values and BIC percentages.

Implant design
In **Study I**, it was found that many of the implants failed to integrate. A possible reason for this is the implant design. Initial implant stability has been described in the literature as being lower for a cylindrical implant design than for a threaded implant (31).

Initial implant stability is important for successful osseointegration (144). When movement occurs between the implant and bone, normal bone healing is negatively affected, and instead of bone the implant will be encapsulated in fibrous tissue, eventually leading to implant loss (145). Implant design and surgical technique are two factors that influence the primary stability of implants (31), and these factors must be managed correctly in order to avoid soft/fibrous tissue formation. To ensure good initial stability, threaded implants were used in **Study II**.

Surface roughness and bone formation
Besides the macro-structure of the material, the surface topography determines the tissue reaction to the implant (137). The surface roughness measurements from **Study I** show that the cylinder shaped nanoHA-coated test implants were smoother than the uncoated control implants at the micrometer level. This may be a consequence of the nanoHA-coating procedure, which involves a treatment process at 300°C that may create a smoother surface due to sintering. An alternative explanation for the smoother surface is that the nanoHA evens out the underlying structure at the micrometer level. Despite the smoother

micro-roughness (though not statistically significant), higher mean values for the histomorphometric parameters were observed for the nanoHA-coated implants. This may indicate the importance of the nano-structure of HA. The AFM showed similar level of nano-roughness (Sa) for the test and control, although the nanoHA-coated implants had a more densely peaked roughness (Sds) than the control implants.

In **Study II**, the results from the surface topography analysis were rather similar for the test and control materials. However, the nanoHA-coated test implants showed somewhat higher values for all the surface parameters, as compared to the uncoated control implants (not statistically tested).

The Sa values were <1 μm for all the PEEK implants (test and control). These surfaces are considered as smooth (<0.5 μm) or minimally rough (0.5–1.0 μm) at the micrometer level. It has been shown, for titanium implants with a moderately rough surface (Sa value of approximately 1.5 μm), produces an enhanced bone response (146).

Our starting hypothesis was that the nano-sized HA coating would enhance osseointegration, as it has been shown that nanoHA on titanium implants improves bone healing (67). The HA used in **Studies I** and **II** was synthesized according to a soft-template method that creates nano-sized apatite on the surface, which resembles the apatite in bone tissue (147). It has been suggested that the bioactivity of HA is due to the ion-exchange reactions that occur at the bone-implant interface creating a "biologically equivalent apatitic surface on the implanted material" (148). The enhanced bone healing has been attributed not only to the surface chemistry conferred by the HA, but also to the nanometer-scale structures. Meirelles et al. removed the microstructure on implants in order to investigate the effects of nanoparticles (67). They observed improved bone healing on the electro-polished surfaces that were coated with nanoHA particles, as compared to uncoated implants, although they could not determine if this was an effect of chemistry or nanotopography. It has been proposed by others that nanometer-sized particles accelerate bone formation by facilitating the adhesion of osteoblasts to the implant surface (149). NanoHA has been applied on titanium implants, rendering an improved bone response (62). However, another study using the same coating did not report any enhancement of osseointegration (68). Even though there was a greater bone response to nanoHA-coated implants in the two studies of this thesis, it remains unclear as to whether this is an effect of the nanostructure, of the HA or a synergistic effect of both the nanostructure and the HA.

Biomechanical tests

The RTQ test applied in **Study II** to test the integration between the implants and the bone tissue, showed significantly higher values for the test implants than for the control implants. The higher RTQ values reflect stronger biomechanical bonding between the nanoHA-coated PEEK implants and the bone tissue, resulting in improved osseointegration. Other studies have also demonstrated positive correlations between RTQ values and histomorphometric bone-contact measurements (5). While histomorphometric measurements (e.g., BIC and BA) provide a two-dimensional representation of the implant and surrounding tissue in a specific position (usually the center of the implant), the RTQ test render a three-dimensional representation of the loosening torque in Ncm. It is possible to convert the results to shear strength (N/mm^2) data, but for that, one need to know the bone-implant contact (150); however, this was not performed in the present study.

In the study of Johansson et al., threaded screw-shaped PEEK implants were inserted in the tibial bones of 24 rabbits (36). Half of the implants were coated with nanoHA using the same spin-coating technique as used in **Studies I** and **II**. The nanoHA-coated implants showed higher RTQ values after 3 and 12 weeks of healing, as compared to the uncoated PEEK implants. Their results are consistent with the results obtained in **Study II** of this thesis. However, in the study performed by Johansson and colleagues, the RTQ values were lower after 12 weeks than after 3 weeks (not statistically tested) for both the test and control implants. While the authors of that study could not explain this finding, they suggested that the effect of the nanoHA coating was primarily on the mineralization of bone at the early stage of healing.

Histomorphometric analysis

The histomorphometric results from **Study I** showed no differences between the nanoHA-coated PEEK implants and the uncoated PEEK control implants. The nanoHA-coated implants had higher mean values for BIC and BA, although the differences were not statistically significant. Since several of the implants were lost, a limited number of samples were examined histomorphometrically. Thus, the nonsignificant result may be due to the low number of samples involved in the study.

The increased osseointegration of the nanoHA-coated implants observed in **Study II** was confirmed by both the higher RTQ values and the histomorphometric results. The histomorphometric analysis showed significantly higher BIC percentages for the test than for the control implants after 6 weeks of healing. There were no differences between the groups in terms of BA when measured in all threads. However, a comparison of the three

best consecutive threads revealed significantly higher BA values in the test implant group.

The BA quantification was performed using a semi-automatic software (141). This software categorizes the pixels of the histologic images as: bone tissue, non-bone tissue or implant. Subsequently, the BA in regions of interest is quantified objectively, which can eliminate the variation that may occur between different observers. However, it should be noted that measurements made with this software can render over- or underestimations due to for example staining artifacts, even if it is possible to make manual corrections after the measurement is performed.

In the histological sections, it was difficult to observe osteoblasts on the osteoid rim and osteoclasts resorbing bone. The reason for this is not clear however such cells are observed in relation to integration of metal implants. It is known that pH play a role in bone remodeling (151). Due to surgery and implant insertion as well as implant material one can speculate *if* and *how* pH may change during the follow up time. From results based on metal implants inserted in rabbit bone it is well known that c.p. titanium implants osseointegrate to a higher degree compared to implants made of Ti6Al4V (152). Is this a reason related to a "positive foreign body reaction" due to the implant-material used?

Some interesting subjects to further investigate could be; What was the pH in the interface at the time of insertion and did it change during the follow up time? Was the pH "out of balance" and thus a factor leading to lack of osteoblasts on the osteoid rims? In the present thesis these issues were not controlled. However, in future studies such will be a challenged to involve and by doing so we may enhance our understanding for the complexity of spare part integration/non-integration in vivo.

As mentioned, the process of healing that occurs around an implant is complex. Not only do the "hard factors" (material, design and surface, which are "controllable") govern the integration, but also the "soft factors" have impacts. These soft factors (surgical technique, host tissue, and loading conditions) are even more complex and more difficult to control than the hard factors. Observations made for implants in animal models do not necessarily hold true for implants in human bone. Thus, screening of implants at various levels is crucial before the novel material is introduced on the market. A CE-marked implant does not mean that the implant has been tested in the appropriate environment/tissue in which it could be used. Instead, it is only tested according to standards related to the material properties. Thus, it is not ready

for clinical usage before adequate in vivo pre-clinical tests have been performed and evaluated. Some of the industrial standards may need to be upgraded so as to include "more complex issues" related to the biocompatibility of various biomaterials and the two-way process, i.e., the interactions between the material and tissue (30).

5.2 STUDY III

The objectives of **Study III** were to investigate how cytokine release from PBMCs is affected when in contact with the different materials, i.e., machined Ti6Al4V and PEEK, as well as blasted PEEK, and the impacts of material surface roughness on cell adherence and cytokine release.

The results show that pro-inflammatory cytokines are released at higher levels from PBMCs that are in contact with the PEEK surfaces than from PBMCs that are exposed to machined Ti6Al4V. Moreover, the rougher PEEK surface induce even higher levels of pro-inflammatory cytokines from the PBMCs than the does the machined PEEK surface. Therefore, the composition, surface chemistry, and topography of the implant material all exert influence on the release of cytokines from implant-attached PBMCs.

Cytokines
Inflammation is closely associated with the formation of tissues around the implant (79, 80). Cytokines, chemokines, and growth factors, which are important regulators of cell migration and growth, are involved in the interactions between the surrounding tissues and the implanted material. The release of these signaling molecules from monocytes and lymphocytes is influenced in different ways by the different biomaterials (153).

In the present study, the Bio-Plex Pro assay was used to measure the levels of cytokines released from cells that were exposed to the tested materials. It is a challenge to interpret these data because cytokines exert diverse effects on leukocytes (as well as on other cell types) (88). Therefore, a commonly used strategy is to investigate in detail the pro-inflammatory cytokines, given that these cytokines appear to play important roles in the early inflammatory responses to the implant materials and could therefore affect the clinical outcome (154).

Significantly higher levels of IL-1β, IL-4, IL-6, TNF-α, and IFN-γ were secreted by the PBMCs exposed to the machined (smooth) PEEK and the blasted PEEK than by the PBMCs that were exposed to Ti6Al4V. Furthermore, the secretion levels of these cytokines were significantly higher upon exposure

of the PBMCs to blasted PEEK than to machined PEEK. In vitro studies have shown that macrophages that are in contact with an implant material during wound healing are stimulated to secrete pro-inflammatory cytokines (153).

Even though pro-inflammatory cytokines are associated with activation of the inflammatory responses of the host, different cytokines can drive diverse pathways. IFN-γ activates the classical M1 macrophage phenotype that kills microorganisms, upregulates pro-inflammatory cytokines, and inhibits anti-inflammatory cytokines (77). However, IL-4 stimulates the alternatively activated M2 macrophages that inhibit other pro-inflammatory cytokines and promote the release of anti-inflammatory cytokines (77). Therefore, it has been suggested that macrophages that adhere to biomaterials are associated with a phenotypic switch from M1 to M2, since IL-4 induces the formation of FBGCs (or MNGCs) (79, 80).

An additional aspect, not studied in this thesis, is to examine the induction by the implant materials of anti-inflammatory cytokines, such as IL-10 and transforming growth factor (TGF)-β. Both IL-10 (155) and TGF-β (156) are known to inhibit osteoclastic bone resorption.

Surface roughness and inflammation

In the present thesis, it is shown that cytokine release from implant-attached PBMCs is not only affected by the compositions of the different materials, but also that by the roughness of the material surfaces at the micrometer scale. In general, the levels of cytokines secreted by the PBMCs were significantly higher in response to the blasted PEEK than to the machined PEEK, which in turn were higher than those in response to the machined Ti6Al4V. This implicates the importance of surface morphology and surface chemistry on the effects on cellular responses in vitro. The results of this study are consistent with the findings of previous studies: surface topography plays a role in cytokine release from inflammatory cells (157, 158). This may be attributed to the fact that the attachment of inflammatory cells increases with surface roughness (159).

In the present study, we observed linkages between the number of PBMCs attached to the implant surface, the levels of release of certain pro-inflammatory cytokines, and the roughness of the implant surface. Thus, the numbers of cells attached to the different surfaces appear to correlate with the observed patterns of cytokine secretion. However, further studies are needed to clarify this issue.

In the present study, we did not detect any difference in the numbers of attached PBMCs between the machined PEEK and the blasted PEEK, even though the PBMCs that adhered to the blasted PEEK showed higher levels of cytokine release. A possible reason for this is that the confocal microscopy used to visualize the attached cells operates on a single focal plane. This means that it is not possible to detect cells above or below the focal plane with this method. Therefore, the actual number of cells on the blasted PEEK might be higher than detected (which is more likely on a rougher surface than on a smooth one). To avoid this limitation, one can use z-stack imaging to capture 3D pictures of the cells attached to the surface (160). However, due to the background signal from the polymer (i.e., PEEK) surface, it was difficult to distinguish the cells closest to the surface. Therefore, it was not possible to quantify the cells with z-stack imaging in this study. Nonetheless, the obtained z-stack images revealed the morphologies of the cells in the vicinity of the surfaces (Figure 18). Thus, this method is interesting to explore further in coming studies.

In the study conducted by Olivares-Navarette and coworkers, the concentrations of pro-inflammatory cytokines released after exposure of cells to PEEK and to Ti6Al4V with different levels of surface roughness were compared (40). When human mesenchymal stem cells were cultured for 7 days on PEEK disks and Ti6Al4V disks there was increased secretion of pro-inflammatory cytokines in response to PEEK, as compared to the titanium alloy. The results obtained accorded with those in the present study. Olivares-Navarette and colleagues (40) have suggested that these cytokines enhance fibrous tissue formation, which may explain why fibrosis is detected histologically around PEEK implants, as opposed to the peri-implant bone formation observed around titanium alloys (37). The release of pro-inflammatory mediators indicates that the PEEK material induces stronger inflammation than does Ti6Al4V, and that the macrophage response varies depending on the material used in the implant. Thus, it has been shown that both the surface chemistry and morphology of a biomaterial affect the cytokine expression patterns (85), which are consistent with the results from **Study III** in this thesis.

Inflammation

Since macrophages are involved in both the integration (161) and failure (162) of implants, it is not clear whether the exacerbated inflammatory response is beneficial or detrimental in the clinical situation. Since the pro-inflammatory cytokines are involved in the inflammatory process, they may also be involved in disease and in causing osteolysis (bone resorption around implants). IL-1 and TNF can stimulate osteoclast development, which can lead to bone

resorption and implant failure, which is of clinical relevance (163, 164). However, inflammation is an inevitable response of the host when implants are inserted, and it is also part of normal wound healing.

Trindade et al. have shown that titanium implants inserted in rabbit bone induce an inflammatory environment that favors bone formation (165). They have suggested that when a foreign body is identified in the bone tissue the immune system contributes to the development of a bone-forming environment, to encapsulate the implant in bone tissue. In another in vivo study by the same research group, they have shown that this inflammatory reaction to a foreign body is material-specific and is affected by the surface topography (166). It has been shown that titanium displays stronger M2 (reparative) anti-inflammatory regulation, while copper and PEEK exhibit a mixture of M1 (pro-inflammatory) and M2-phenotypes. This may explain the success of osseointegration around pure titanium but not around other materials.

The results from **Study III** clearly show that PEEK induces a stronger inflammatory response than Ti6Al4V. These results are of interest, as this information may be of importance when using PEEK materials in medical devices and, as mentioned previously, a stronger inflammatory response may impair bone healing around implants. Furthermore, the results of this study improve our understanding of the host reactions to biomaterials and how their characteristics may affect biocompatibility.

5.3 STUDY IV

The results of this in vitro study show that there are significant differences in the bacterial growth patterns when the bacteria are exposed to the different materials. Our original hypothesis was that biofilm formation would be affected by the compositions and roughness levels of various materials. However, the results obtained show that the tested bacteria grow well on all the materials.

Surface roughness and biofilm formation

It is confirmed that surface roughness has an impact on the adhesion of bacteria to these materials. When comparing the effects of material and time, the formation of a biofilm by *S. sanguinis* is significantly higher on PEEK and blasted PEEK than on Ti6Al4V. Moreover, *S. oralis* grows better on the blasted PEEK than on any of the other materials. The same tendency is observed for *S. gordonii*, in that the blasted PEEK supports a significantly higher level of biofilm formation than does the non-blasted PEEK, both in the presence and absence of sucrose.

It is known that a rougher surface supports higher numbers of bacteria in the biofilm than does a smoother surface (118). One reason for this is that the bacteria adhere more easily and become sheltered in the micrometer-scale cracks in the rougher surface (117).

Since the blasted PEEK shows stronger biofilm formation compared to the other materials in **Study IV**, it can be concluded that it is preferable to use materials with smoother surfaces (i.e., PEEK, cp-Ti or TiAl6V4) when the goal is to decrease the level of biofilm formation on the implant surface.

Wettability and biofilm formation

The wettability of a biomaterial has been proposed to influence biofilm formation (167). Materials that have a higher surface free energy create a more-wettable surface and are more likely to allow the adherence of bacteria (118), although this also depends on the hydrophobicity of the bacteria (168). In the present study, the blasted PEEK had the highest contact angle (least-wettable), followed by machined PEEK. *S. sanguinis* and *S. oralis* are reported to be hydrophobic and have previously been shown to adhere preferentially to hydrophobic surfaces (168). This explains in part their apparent affinity for blasted PEEK surfaces, in addition to the surface roughness.

Chemical composition and biofilm formation

The chemical composition of the surface of a material may also play a role in biofilm formation (169). The attachment of bacteria to different surfaces involves complex mechanisms with different chemo-physical forces that attract or repel bacteria (118). There are only a few published studies on bacterial growth related to the effect of the surface chemistry of PEEK. Since surface composition and roughness both influence wettability, it is difficult to decide which is the most influential. However, even though the degree of wettability and surface roughness interact with each other, it has been suggested that surface roughness is the more important of these two parameters (170).

The findings from **Study IV** suggest that smooth PEEK is no more susceptible to bacterial colonization than is cp-Ti or TiAl6V4. From this perspective, PEEK is a suitable alternative to metals as a prosthetic material. Similar results have been obtained when comparing the biofilm formation abilities of *S. aureus* and *S. epidermidis* on PEEK and titanium (Rochford et al. 2014). In the present study, similar levels of growth of *S. sanguinis*, *S. oralis*, and *S. gordonii* were observed on cp-Ti and Ti6Al4V. This was expected, since these two materials have similar degrees of roughness and wettability (171), and is consistent with the results for *S. sanguinis* reported previously (172).

Significantly increased growth of *E. faecalis* was observed on the cp-Ti surface compared to the other three surfaces. To date, the limited number of in vitro studies comparing bacterial growth on cp-Ti and Ti6Al4V have shown inconsistent results, depending on the bacterial species tested and the study design. The discrepant results may also reflect the heterogeneity of the cell wall properties of subpopulations of cells within a single-species bacterial population, as reported for *E. faecalis* (173). In a review article, Shah et al (174) concluded that there is also a lack of in vivo studies regarding bacterial growth and the differences between cp-Ti and Ti6Al4V.

Saliva

Biomaterials that are introduced into the oral environment are immediately covered with a thin layer of pellicle, which consists of several proteins, enzymes, and other molecules from the saliva, to which bacteria can attach to form a biofilm (118). On the one hand, the saliva facilitates bacterial adhesion, while on the other hand, it contains antibacterial proteins that inhibit bacterial growth and adhesion (175). Furthermore, the pellicle-conditioning film may balance to some extent the differences in the physicochemical surface properties (175). In the present study, the bacteria were not cultured in the presence of saliva, so this effect is not taken into account. Another important aspect to consider is that biofilms within dental plaque do not consist of a single species but rather the build-up of communities in which several different species interact in a complex manner and respond to environmental changes as a single unit (176). Even though individual species were examined separately in the present study, the early colonizers *S. sanguinis*, *S. oralis*, and *S. gordonii* are of importance because they enable the attachment of subsequent colonizers and thereby influence the composition of the maturing biofilm. To examine biofilm formation by *E. faecalis* is also of interest as it is a highly virulent bacterium with the ability to produce biofilms on various medical devices (114, 177).

6 CONCLUSIONS

NanoHA-coated, cylinder shaped and threaded PEEK implants manifest improved bone formation, as compared to uncoated implants after 6 weeks of follow-up.

PEEK induces a stronger inflammatory response from PBMCs than does Ti6Al4V. The surface chemistry, and topography of the implant material influence the magnitude of release of cytokines from implant-attached PBMCs.

The levels of bacterial adhesion to PEEK, cp-Ti and Ti6Al4V are similar. However, blasted PEEK, which has a rougher surface topography than the other materials, supports greater biofilm formation by oral bacterial species.

Within the limitations of the methods used in the present thesis, it can be concluded that PEEK holds promise as a material that can be used in various dental applications.

7 FUTURE PERSPECTIVES

As mentioned in the *Introduction* section, it seems unlikely that PEEK will replace titanium as a material for dental implants, considering the successful outcome achieved with titanium implants to date. However, since PEEK has favorable mechanical and biocompatibility properties, several potential uses for PEEK can be envisaged in metal-free constructions in the field of dentistry.

Methacrylate based materials (e.g., PMMA) are used in many prosthetic applications, such as removable dentures and long-term provisional bridges, and in combination with metals, as in supra-constructions for implant-supported bridges. These methacrylates are known to leak residual monomers that can have cytotoxic effects and cause inflammation in the host tissue.

Since PEEK is a chemically stable polymer, it may replace methacrylates that are extensively used in prosthetic dentistry (e.g., denture base materials). PEEK-containing materials have already attracted interest from the dental implant industry where many products made of PEEK are used, for example in healing abutments, long-term implant-supported crowns and scan bodies for intra-oral scanning. In these contexts, PEEK may become the material of choice, not only because of its good biocompatibility profile and mechanical features, but also due to the possibility to fabricate PEEK restorations with CAD/CAM techniques, thereby creating a digital workflow that is both time- and cost-efficient.

This thesis provides the basis for further research on PEEK materials in dental applications. There is a need to investigate the performance of PEEK in mechanical assessments in the context of dental materials. Additional in vivo studies, such as soft tissue experiments, should be conducted to evaluate the biocompatibility of PEEK as a healing abutment. Finally, clinical trials are needed to evaluate the performance of PEEK in restorative dentistry. The acquired information will be important in ensuring the use of suitable materials in dental devices.

ACKNOWLEDGMENTS

I wish to express my deepest gratitude to all who made this thesis possible.

I would like to thank:

Victoria Stenport, my main supervisor, for being an excellent mentor. I have had the privilege to work with you day to day and I am so grateful that you always make the time to discuss research issues, giving useful criticisms and sharing your knowledge or just talking about matters of everyday life. Thank you for all your guidance, support, and help during all these years.

Carina B. Johansson, my co-supervisor, for generously sharing your time and wisdom, for all the interesting discussions, and for sagely scrutinizing this thesis. You have taught me how to review research in a critical manner and given me valuable knowledge of histology and material science.

Ann Wennerberg, my co-supervisor, for introducing me to the field of research and for inspiring me to continue with the project that you initiated.

Anna-Karin Östberg, for all your help in carrying out the cytokine study, and for always taking the time to explain the experimental methods.

Sebastian Franco-Tabares, for all your help, especially with the surface evaluations.

Petra H. Johansson and **Maria Hoffman**, for your assistance and knowledge in the laboratory and for always being helpful.

Rachel Sammons and all the other people at the University of Birmingham, for working together on the last study. Thank you for your warm hospitality during my stay in Birmingham.

Per Kjellin and all the staff at Promimic, for a great collaboration.

All my co-authors, for your hard work and providing knowledge on our projects.

Kostas Bougas, for being a great friend over many years and for kindly helping me with the surface analysis.

Ryo Jimbo and **Pär Johansson** for collaboration on our shared projects.

Adad Baranto, for giving me the opportunity to observe spinal surgery using PEEK implants.

Torgny Alstad, for helping me to understand the statistical analysis.

Maria Smedh at the Centre for Cellular Imaging at the University of Gothenburg and the National Microscopy Infrastructure, NMI (VR-RFI 2016-00968) for providing assistance in microscopy.

Johan Thompson, for your help with the graphical design.

Katarina Nobelius, for being helpful with the administration.

Jan Kowar, for your friendship. We have had some memorable trips.

Malin Olsson Malm, my previous "roommate", for interesting discussions.

All fellow PhD students at the department. I wish you good luck with your projects.

Torsten Jemt, for sharing your wisdom, for inspiring discussions, and for teaching me how to evaluate research.

Bertil Friberg, for help with designing the test samples, for being a good mentor, and for constantly encouraging me. I will always be grateful to you.

Bettina Aglöv, for being a great colleague and friend. It's a true pleasure to work with you.

The staff and my colleagues at the **Department of Prosthodontics/Dental Materials Science** and the staff at the **Brånemark Clinic**, for all your support.

The entire **Staifo family** for your endless generosity. I am so grateful for your help and support.

All **my friends** for the support.

My loving sisters **Brigitte**, **Belgin**, and **Tibella**, for all your support.

My mother Seydi, my greatest role model, for your guidance in life. You are truly an inspiration.

My three fantastic children, **Tigris**, **Ninve** and **Ilona**, for fulfilling my life. You are my everything.

Imra, my best friend and partner in life. For always believing in me and for your unfailing patience. This would not have been possible without you. I love you endlessly.

Funding
The studies in this thesis were supported by grants from the Hjalmar Svensson Research Foundation, the Wilhelm and Martina Lundgren Science Foundation, Sigge Perssons & Alice Nybergs stiftelse (Gothenburg Dental Society), Adlerbert Research Foundation, the Sylvan Foundation, the Royal Society of Arts and Sciences in Gothenburg, the Public Dental Health Care Service (region of Västra Götaland), and the Nanoscience and Nanotechnology Area of Advance at Chalmers University of Technology.

REFERENCES

1. Kurtz SM. An Overview of PEEK Biomaterials. PEEK Biomaterials Handbook: Elsevier; 2012.
2. Williams DF. Definitions in Biomaterials: Proceedings of a Consensus Conference of the European Society for Biomaterials, Chester, Engl., March 3-5, 1986: Elsevier; 1987.
3. NIH Consens Statement Online Clinical Applications of Biomaterials. 1982;4(5):1-19.
4. Love B. Polymeric Biomaterials. In: Love B, editor. Biomaterials: Academic Press; 2017. p. 205-38.
5. Johansson CB. On tissue reactions to metal implants [Thesis]: University of Gothenburg, Gothenburg, Sweden; 1991.
6. Prasad K, Bazaka O, Chua M, Rochford M, Fedrick L, Spoor J, et al. Metallic Biomaterials: Current Challenges and Opportunities. Materials (Basel, Switzerland). 2017;10(8).
7. Anusavice KJ, Phillips RW. Phillips' science of dental materials, ,11th Edition. St. Louis, Mo.: Saunders; 2003.
8. Gautam R, Singh RD, Sharma VP, Siddhartha R, Chand P, Kumar R. Biocompatibility of polymethylmethacrylate resins used in dentistry. J Biomed Mater Res B Appl Biomater. 2012;100(5):1444-50.
9. Chaves CA, Machado AL, Vergani CE, de Souza RF, Giampaolo ET. Cytotoxicity of denture base and hard chairside reline materials: a systematic review. J Prosthet Dent. 2012;107(2):114-27.
10. Niinomi M. Mechanical properties of biomedical titanium alloys. Materials Science and Engineering: A. 1998;243(1-2):231-6.
11. Kurtz SM, Devine JN. PEEK biomaterials in trauma, orthopedic, and spinal implants. Biomaterials. 2007;28(32):4845-69.
12. Gardner SHI. An investigation of the structure-property relationships for high performance thermoplastic matrix, carbon fiber composites with a tailored polyimide interphase: Virginia Tech; 1998.
13. Harsha AP, Tewari US. The Effect of Fibre Reinforcement and Solid Lubricants on Abrasive Wear Behavior of Polyetheretherketone Composites. Journal of Reinforced Plastics and Composites. 2003;22(8):751-67.
14. Lee WT, Koak JY, Lim YJ, Kim SK, Kwon HB, Kim MJ. Stress shielding and fatigue limits of poly-ether-ether-ketone dental implants. J Biomed Mater Res B Appl Biomater. 2012;100(4):1044-52.
15. Bayraktar HH, Morgan EF, Niebur GL, Morris GE, Wong EK, Keaveny TM. Comparison of the elastic and yield properties of human femoral trabecular and cortical bone tissue. J Biomech. 2004;37(1):27-35.
16. PEEK-OPTIMA Natural. Invibio Biomaterial Solutions, Lancashire, UK.
17. PEEK-OPTIMA 30% Carbon fiber-reinforced. Invibio Biomaterial Solutions, Lancashire, UK.
18. Najeeb S, Zafar MS, Khurshid Z, Siddiqui F. Applications of polyetheretherketone (PEEK) in oral implantology and prosthodontics. J Prosthodont Res. 2016;60(1):12-9.
19. Schwitalla AD, Spintig T, Kallage I, Muller WD. Flexural behavior of PEEK materials for dental application. Dent Mater. 2015;31(11):1377-84.

20. International Organization for Standardization. ISO 10477:2018. Dentistry — Polymer-based crown and veneering materials2017.
21. Kurtz SM. An Overview of PEEK Biomaterials. PEEK Biomaterials Handbook: Elsevier; 2012. p. 9-22.
22. Boinard E, Pethrick R, MacFarlane C. The influence of thermal history on the dynamic mechanical and dielectric studies of polyetheretherketone exposed to water and brine. Polymer. 2000;41(3):1063-76.
23. Zhang G, Latour RA, Jr., Kennedy JM, Del Schutte H, Jr., Friedman RJ. Long-term compressive property durability of carbon fibre-reinforced polyetheretherketone composite in physiological saline. Biomaterials. 1996;17(8):781-9.
24. Cole K, Casella I. Fourier transform infra-red spectroscopic study of thermal degradation in poly (ether ether ketone)-carbon composites. Polymer. 1993;34(4):740-5.
25. Brown SA, Hastings RS, Mason JJ, Moet A. Characterization of short-fibre reinforced thermoplastics for fracture fixation devices. Biomaterials. 1990;11(8):541-7.
26. Li HM, Fouracre RA, Given MJ, Banford HM, Wysocki S, Karolczak S. The effects on polyetheretherketone and polyethersulfone of electron and /spl gamma/ irradiation. IEEE Transactions on Dielectrics and Electrical Insulation. 1999;6(3):295-303.
27. Brantigan JW, Steffee AD. A carbon fiber implant to aid interbody lumbar fusion. Two-year clinical results in the first 26 patients. Spine (Phila Pa 1976). 1993;18(14):2106-7.
28. Baidya KP, Ramakrishna S, Rahman M, Ritchie A. Quantitative radiographic analysis of fiber reinforced polymer composites. J Biomater Appl. 2001;15(3):279-89.
29. Williams DF. Progress in Biomedical Engineering, Vol. 4. Definitions in Biomaterials: Elsevier, Amsterdam; 1987.
30. Williams DF. The Williams Dictionary of Biomaterials Liverpool, UK: Liverpool. University Press; 1999.
31. Albrektsson T, Branemark PI, Hansson HA, Lindstrom J. Osseointegrated titanium implants. Requirements for ensuring a long-lasting, direct bone-to-implant anchorage in man. Acta Orthop Scand. 1981;52(2):155-70.
32. Williams DF. There is no such thing as a biocompatible material. Biomaterials. 2014;35(38):10009-14.
33. Katzer A, Marquardt H, Westendorf J, Wening JV, von Foerster G. Polyetheretherketone--cytotoxicity and mutagenicity in vitro. Biomaterials. 2002;23(8):1749-59.
34. Jockisch KA, Brown SA, Bauer TW, Merritt K. Biological response to chopped-carbon-fiber-reinforced peek. J Biomed Mater Res. 1992;26(2):133-46.
35. Barkarmo S, Andersson M, Currie F, Kjellin P, Jimbo R, Johansson CB, et al. Enhanced bone healing around nanohydroxyapatite-coated polyetheretherketone implants: An experimental study in rabbit bone. J Biomater Appl. 2014;29(5):737-47.
36. Johansson P, Jimbo R, Kozai Y, Sakurai T, Kjellin P, Currie F, et al. Nanosized Hydroxyapatite Coating on PEEK Implants Enhances Early Bone Formation: A

Histological and Three-Dimensional Investigation in Rabbit Bone. Materials (Basel, Switzerland). 2015;8(7):3815-30.
37. Toth JM, Wang M, Estes BT, Scifert JL, Seim HB, 3rd, Turner AS. Polyetheretherketone as a biomaterial for spinal applications. Biomaterials. 2006;27(3):324-34.
38. Olivares-Navarrete R, Hyzy SL, Gittens RA, Schneider JM, Haithcock DA, Ullrich PF, et al. Rough titanium alloys regulate osteoblast production of angiogenic factors. Spine J. 2013;13(11):1563-70.
39. Nemoto O, Asazuma T, Yato Y, Imabayashi H, Yasuoka H, Fujikawa A. Comparison of fusion rates following transforaminal lumbar interbody fusion using polyetheretherketone cages or titanium cages with transpedicular instrumentation. Eur Spine J. 2014;23(10):2150-5.
40. Olivares-Navarrete R, Hyzy SL, Slosar PJ, Schneider JM, Schwartz Z, Boyan BD. Implant materials generate different peri-implant inflammatory factors: poly-ether-ether-ketone promotes fibrosis and microtextured titanium promotes osteogenic factors. Spine (Phila Pa 1976). 2015;40(6):399-404.
41. Najeeb S, Khurshid Z, Zohaib S, Zafar MS. Bioactivity and Osseointegration of PEEK Are Inferior to Those of Titanium: A Systematic Review. 2016;42(6):512-6.
42. Abu Bakar MS, Cheng MH, Tang SM, Yu SC, Liao K, Tan CT, et al. Tensile properties, tension-tension fatigue and biological response of polyetheretherketone-hydroxyapatite composites for load-bearing orthopedic implants. Biomaterials. 2003;24(13):2245-50.
43. Ha SW, Mayer J, Koch B, Wintermantel E. Plasma-sprayed hydroxylapatite coating on carbon fibre reinforced thermoplastic composite materials. J Mater Sci Mater Med. 1994;5(6):481-4.
44. Hench LL, Splinter RJ, Allen W, Greenlee TJJobmr. Bonding mechanisms at the interface of ceramic prosthetic materials. 1971;5(6):117-41.
45. Lee JJ, Rouhfar L, Beirne OR. Survival of hydroxyapatite-coated implants: a meta-analytic review. J Oral Maxillofac Surg. 2000;58(12):1372-9; discussion 9-80.
46. Tengvall P, Skoglund B, Askendal A, Aspenberg P. Surface immobilized bisphosphonate improves stainless-steel screw fixation in rats. Biomaterials. 2004;25(11):2133-8.
47. Malekzadeh B, Tengvall P, Ohrnell LO, Wennerberg A, Westerlund A. Effects of locally administered insulin on bone formation in non-diabetic rats. Journal of biomedical materials research Part A. 2013;101(1):132-7.
48. Bougas K, Jimbo R, Vandeweghe S, Hayashi M, Bryington M, Kozai Y, et al. Bone apposition to laminin-1 coated implants: histologic and 3D evaluation. Int J Oral Maxillofac Surg. 2013;42(5):677-82.
49. Arvidsson A, Franke-Stenport V, Andersson M, Kjellin P, Sul YT, Wennerberg A. Formation of calcium phosphates on titanium implants with four different bioactive surface preparations. An in vitro study. J Mater Sci Mater Med. 2007;18(10):1945-54.
50. Altankov G, Grinnell F, Groth T. Studies on the biocompatibility of materials: fibroblast reorganization of substratum-bound fibronectin on surfaces varying in wettability. J Biomed Mater Res. 1996;30(3):385-91.

51. Lim JY, Shaughnessy MC, Zhou Z, Noh H, Vogler EA, Donahue HJ. Surface energy effects on osteoblast spatial growth and mineralization. Biomaterials. 2008;29(12):1776-84.
52. Garcia AJ, Keselowsky BG. Biomimetic surfaces for control of cell adhesion to facilitate bone formation. Crit Rev Eukaryot Gene Expr. 2002;12(2):151-62.
53. Ha SW, Kirch M, Birchler F, Eckert KL, Mayer J, Wintermantel E, et al. Surface activation of polyetheretherketone (PEEK) and formation of calcium phosphate coatings by precipitation. J Mater Sci Mater Med. 1997;8(11):683-90.
54. Rao PJ, Pelletier MH, Walsh WR, Mobbs RJ. Spine interbody implants: material selection and modification, functionalization and bioactivation of surfaces to improve osseointegration. Orthop Surg. 2014;6(2):81-9.
55. Cheng BC, Koduri S, Wing CA, Woolery N, Cook DJ, Spiro RC. Porous titanium-coated polyetheretherketone implants exhibit an improved bone-implant interface: an in vitro and in vivo biochemical, biomechanical, and histological study. Medical devices (Auckland, NZ). 2018;11:391-402.
56. Sunarso, Tsuchiya A, Fukuda N, Toita R, Tsuru K, Ishikawa K. Effect of micro-roughening of poly(ether ether ketone) on bone marrow derived stem cell and macrophage responses, and osseointegration. J Biomater Sci Polym Ed. 2018;29(12):1375-88.
57. Wu GM, Hsiao WD, Kung SF. Investigation of hydroxyapatite coated polyether ether ketone composites by gas plasma sprays. Surface and Coatings Technology. 2009;203(17–18):2755-8.
58. Lee JH, Jang HL, Lee KM, Baek HR, Jin K, Hong KS, et al. In vitro and in vivo evaluation of the bioactivity of hydroxyapatite-coated polyetheretherketone biocomposites created by cold spray technology. Acta Biomater. 2013;9(4):6177-87.
59. Rabiei A, Sandukas S. Processing and evaluation of bioactive coatings on polymeric implants. Journal of biomedical materials research Part A. 2013.
60. Ellies LG, Carter JM, Natiella JR, Featherstone JD, Nelson DG. Quantitative analysis of early in vivo tissue response to synthetic apatite implants. J Biomed Mater Res. 1988;22(2):137-48.
61. Gottlander M, Albrektsson T, Carlsson LV. A histomorphometric study of unthreaded hydroxyapatite-coated and titanium-coated implants in rabbit bone. Int J Oral Maxillofac Implants. 1992;7(4):485-90.
62. Jimbo R, Coelho PG, Bryington M, Baldassarri M, Tovar N, Currie F, et al. Nano hydroxyapatite-coated implants improve bone nanomechanical properties. J Dent Res. 2012;91(12):1172-7.
63. Suska F, Omar O, Emanuelsson L, Taylor M, Gruner P, Kinbrum A, et al. Enhancement of CRF-PEEK osseointegration by plasma-sprayed hydroxyapatite: A rabbit model. J Biomater Appl. 2014.
64. Barkarmo S, Wennerberg A, Hoffman M, Kjellin P, Breding K, Handa P, et al. Nano-hydroxyapatite-coated PEEK implants: a pilot study in rabbit bone. Journal of biomedical materials research Part A. 2013;101(2):465-71.
65. Albrektsson T. Hydroxyapatite-coated implants: a case against their use. J Oral Maxillofac Surg. 1998;56(11):1312-26.
66. Rokkum M, Reigstad A, Johansson CB. HA particles can be released from well-fixed HA-coated stems: histopathology of biopsies from 20 hips 2-8 years after implantation. Acta Orthop Scand. 2002;73(3):298-306.

67. Meirelles L, Arvidsson A, Andersson M, Kjellin P, Albrektsson T, Wennerberg A. Nano hydroxyapatite structures influence early bone formation. Journal of biomedical materials research Part A. 2008;87(2):299-307.
68. Svanborg LM, Hoffman M, Andersson M, Currie F, Kjellin P, Wennerberg A. The effect of hydroxyapatite nanocrystals on early bone formation surrounding dental implants. Int J Oral Maxillofac Surg. 2011;40(3):308-15.
69. Wennerberg A, Albrektsson T. Effects of titanium surface topography on bone integration: a systematic review. Clin Oral Implants Res. 2009;20 Suppl 4:172-84.
70. Ergun C, Liu H, Webster TJ, Olcay E, Yilmaz S, Sahin FC. Increased osteoblast adhesion on nanoparticulate calcium phosphates with higher Ca/P ratios. Journal of biomedical materials research Part A. 2008;85(1):236-41.
71. Gittens RA, McLachlan T, Olivares-Navarrete R, Cai Y, Berner S, Tannenbaum R, et al. The effects of combined micron-/submicron-scale surface roughness and nanoscale features on cell proliferation and differentiation. Biomaterials. 2011;32(13):3395-403.
72. Mendes VC, Moineddin R, Davies JE. The effect of discrete calcium phosphate nanocrystals on bone-bonding to titanium surfaces. Biomaterials. 2007;28(32):4748-55.
73. Jimbo R, Sotres J, Johansson C, Breding K, Currie F, Wennerberg A. The biological response to three different nanostructures applied on smooth implant surfaces. Clin Oral Implants Res. 2012;23(6):706-12.
74. Wennerberg A, Albrektsson T. Structural influence from calcium phosphate coatings and its possible effect on enhanced bone integration. Acta Odontol Scand. 2009;67(6):333-40.
75. Mills CD, Ley K. M1 and M2 macrophages: the chicken and the egg of immunity. J Innate Immun. 2014;6(6):716-26.
76. Selders GS, Fetz AE, Radic MZ, Bowlin GL. An overview of the role of neutrophils in innate immunity, inflammation and host-biomaterial integration. Regenerative biomaterials. 2017;4(1):55-68.
77. Martinez FO, Gordon S. The M1 and M2 paradigm of macrophage activation: time for reassessment. F1000prime reports. 2014;6:13.
78. Omar OM, Graneli C, Ekstrom K, Karlsson C, Johansson A, Lausmaa J, et al. The stimulation of an osteogenic response by classical monocyte activation. Biomaterials. 2011;32(32):8190-204.
79. Franz S, Rammelt S, Scharnweber D, Simon JC. Immune responses to implants–a review of the implications for the design of immunomodulatory biomaterials. Biomaterials. 2011;32(28):6692-709.
80. Anderson JM, Rodriguez A, Chang DT. Foreign body reaction to biomaterials. Semin Immunol. 2008;20(2):86-100.
81. Jones JA, Chang DT, Meyerson H, Colton E, Kwon IK, Matsuda T, et al. Proteomic analysis and quantification of cytokines and chemokines from biomaterial surface-adherent macrophages and foreign body giant cells. J Biomed Mater Res Part A. 2007;83(3):585-96.
82. Miron RJ, Bosshardt DD. Multinucleated Giant Cells: Good Guys or Bad Guys? Tissue engineering Part B, Reviews. 2018;24(1):53-65.
83. Broughton 2nd G, Janis JE, Attinger CE. The basic science of wound healing. Plast Reconstr Surg. 2006;117(7 Suppl):12S-34S.

84. McNally AK, Anderson JM. Interleukin-4 induces foreign body giant cells from human monocytes/macrophages. Differential lymphokine regulation of macrophage fusion leads to morphological variants of multinucleated giant cells. Am J Pathol. 1995;147(5):1487.
85. Östberg A-K, Dahlgren U, Sul Y-T, Johansson CB. Inflammatory cytokine release is affected by surface morphology and chemistry of titanium implants. J Mater Sci Mater Med. 2015;26(4):1-9.
86. Dinarello CA. Proinflammatory cytokines. Chest. 2000;118(2):503-8.
87. Hallab NJ, McAllister K, Brady M, Jarman-Smith M. Macrophage reactivity to different polymers demonstrates particle size-and material-specific reactivity: PEEK-OPTIMA® particles versus UHMWPE particles in the submicron, micron, and 10 micron size ranges. J Biomed Mater Res B Appl Biomater. 2012;100(2):480-92.
88. Rahmat Sam MF, Curran JM, Hunt JA. 4.5 Leukocyte–Biomaterial Interaction In Vitro - Ducheyne, Paul. Comprehensive Biomaterials II. 4. Oxford: Elsevier; 2017. p. 57-69.
89. Scheller J, Chalaris A, Schmidt-Arras D, Rose-John S. The pro- and anti-inflammatory properties of the cytokine interleukin-6. Biochim Biophys Acta. 2011;1813(5):878-88.
90. Manolagas SC. The role of IL-6 type cytokines and their receptors in bone. Ann N Y Acad Sci. 1998;840:194-204.
91. Evans KE, Fox SW. Interleukin-10 inhibits osteoclastogenesis by reducing NFATc1 expression and preventing its translocation to the nucleus. BMC Cell Biol. 2007;8:4.
92. de Waal Malefyt R, Abrams J, Bennett B, Figdor CG, de Vries JE. Interleukin 10(IL-10) inhibits cytokine synthesis by human monocytes: an autoregulatory role of IL-10 produced by monocytes. J Exp Med. 1991;174(5):1209-20.
93. Beutler BA. The role of tumor necrosis factor in health and disease. J Rheumatol Suppl. 1999;57:16-21.
94. Osta B, Benedetti G, Miossec P. Classical and Paradoxical Effects of TNF-alpha on Bone Homeostasis. Front Immunol. 2014;5:48.
95. Flad H-D, Grage-Griebenow E, Scheuerer B, Dürrbaum-Landmann I, Petersen F, Brandt E, et al. The role of cytokines in monocyte apoptosis. Res Immunol. 1998;149(7):733-6.
96. Amstutz HC, Campbell P, Kossovsky N, Clarke IC. Mechanism and clinical significance of wear debris-induced osteolysis. Clin Orthop Relat Res. 1992(276):7-18.
97. Fretwurst T, Nelson K, Tarnow DP, Wang HL, Giannobile WV. Is Metal Particle Release Associated with Peri-implant Bone Destruction? An Emerging Concept. J Dent Res. 2018;97(3):259-65.
98. Pettersson M, Pettersson J, Johansson A, Molin Thoren M. Titanium release in peri-implantitis. J Oral Rehabil. 2019;46(2):179-88.
99. Wennerberg A, Ide-Ektessabi A, Hatkamata S, Sawase T, Johansson C, Albrektsson T, et al. Titanium release from implants prepared with different surface roughness. Clin Oral Implants Res. 2004;15(5):505-12.
100. Pettersson M, Pettersson J, Molin Thoren M, Johansson A. Release of titanium after insertion of dental implants with different surface characteristics - an ex vivo animal study. Acta biomaterialia odontologica Scandinavica. 2017;3(1):63-73.

101. Tawse-Smith A, Ma S, Duncan WJ, Gray A, Reid MR, Rich AM. Implications of Wear at the Titanium-Zirconia Implant-Abutment Interface on the Health of Peri-implant Tissues. Int J Oral Maxillofac Implants. 2017;32(3):599-609.
102. Mabilleau G, Bourdon S, Joly-Guillou ML, Filmon R, Basle MF, Chappard D. Influence of fluoride, hydrogen peroxide and lactic acid on the corrosion resistance of commercially pure titanium. Acta Biomater. 2006;2(1):121-9.
103. Liu A, Richards L, Bladen CL, Ingham E, Fisher J, Tipper JL. The biological response to nanometre-sized polymer particles. Acta Biomater. 2015;23:38-51.
104. Hallab NJ, Jacobs JJ. Chemokines Associated with Pathologic Responses to Orthopedic Implant Debris. Front Endocrinol (Lausanne). 2017;8:5.
105. Stratton-Powell AA, Pasko KM, Brockett CL, Tipper JL. The Biologic Response to Polyetheretherketone (PEEK) Wear Particles in Total Joint Replacement: A Systematic Review. Clin Orthop Relat Res. 2016;474(11):2394-404.
106. Donlan RM. Biofilms: microbial life on surfaces. Emerg Infect Dis. 2002;8(9):881-90.
107. Aas JA, Paster BJ, Stokes LN, Olsen I, Dewhirst FE. Defining the normal bacterial flora of the oral cavity. J Clin Microbiol. 2005;43(11):5721-32.
108. Moons P, Michiels CW, Aertsen A. Bacterial interactions in biofilms. Crit Rev Microbiol. 2009;35(3):157-68.
109. Hojo K, Nagaoka S, Ohshima T, Maeda N. Bacterial interactions in dental biofilm development. J Dent Res. 2009;88(11):982-90.
110. Kolenbrander PE, Palmer Jr RJ, Periasamy S, Jakubovics NS. Oral multispecies biofilm development and the key role of cell–cell distance. Nature Reviews Microbiology. 2010;8(7):471-80.
111. Periasamy S, Kolenbrander PE. Central role of the early colonizer Veillonella sp. in establishing multispecies biofilm communities with initial, middle, and late colonizers of enamel. J Bacteriol. 2010;192(12):2965-72.
112. Kreth J, Merritt J, Qi F. Bacterial and host interactions of oral streptococci. DNA Cell Biol. 2009;28(8):397-403.
113. Øilo M, Bakken V. Biofilm and dental biomaterials. Materials. 2015;8(6):2887-900.
114. Kouidhi B, Zmantar T, Mahdouani K, Hentati H, Bakhrouf A. Antibiotic resistance and adhesion properties of oral Enterococci associated to dental caries. BMC Microbiol. 2011;11(1):155.
115. Busscher H, Rinastiti M, Siswomihardjo W, Van der Mei H. Biofilm formation on dental restorative and implant materials. J Dent Res. 2010;89(7):657-65.
116. Hahnel S, Wieser A, Lang R, Rosentritt M. Biofilm formation on the surface of modern implant abutment materials. Clin Oral Implants Res. 2015;26(11):1297-301.
117. Bollen CM, Lambrechts P, Quirynen M. Comparison of surface roughness of oral hard materials to the threshold surface roughness for bacterial plaque retention: a review of the literature. Dent Mater. 1997;13(4):258-69.
118. Teughels W, Van Assche N, Sliepen I, Quirynen M. Effect of material characteristics and/or surface topography on biofilm development. Clin Oral Implants Res. 2006;17(S2):68-81.
119. Barton AJ, Sagers RD, Pitt WG. Bacterial adhesion to orthopedic implant polymers. J Biomed Mater Res. 1996;30(3):403-10.

120. Rochford E, Poulsson A, Varela JS, Lezuo P, Richards R, Moriarty T. Bacterial adhesion to orthopaedic implant materials and a novel oxygen plasma modified PEEK surface. Colloids and Surfaces B: Biointerfaces. 2014;113:213-22.
121. Panayotov IV, Orti V, Cuisinier F, Yachouh J. Polyetheretherketone (PEEK) for medical applications. J Mater Sci Mater Med. 2016;27(7):118.
122. Cho DY, Liau WR, Lee WY, Liu JT, Chiu CL, Sheu PC. Preliminary experience using a polyetheretherketone (PEEK) cage in the treatment of cervical disc disease. Neurosurgery. 2002;51(6):1343-49; discussion 9-50.
123. Kulkarni AG, Hee HT, Wong HK. Solis cage (PEEK) for anterior cervical fusion: preliminary radiological results with emphasis on fusion and subsidence. Spine J. 2007;7(2):205-9.
124. Lied B, Roenning PA, Sundseth J, Helseth E. Anterior cervical discectomy with fusion in patients with cervical disc degeneration: a prospective outcome study of 258 patients (181 fused with autologous bone graft and 77 fused with a PEEK cage). BMC Surg. 2010;10:10.
125. Scolozzi P, Martinez A, Jaques B. Complex orbito-fronto-temporal reconstruction using computer-designed PEEK implant. J Craniofac Surg. 2007;18(1):224-8.
126. Jokstad A. Computer-assisted technologies used in oral rehabilitation and the clinical documentation of alleged advantages - a systematic review. J Oral Rehabil. 2017;44(4):261-90.
127. Braian M, Jimbo R, Wennerberg A. Production tolerance of additive manufactured polymeric objects for clinical applications. Dent Mater. 2016;32(7):853-61.
128. Stawarczyk B, Beuer F, Wimmer T, Jahn D, Sener B, Roos M, et al. Polyetheretherketone—a suitable material for fixed dental prostheses? J Biomed Mater Res B Appl Biomater. 2013;101(7):1209-16.
129. Lang R, Rosentritt M, Behr M, Handel G. Fracture resistance of PMMA and resin matrix composite-based interim FPD materials. Int J Prosthodont. 2003;16(4):381-4.
130. Costa-Palau S, Torrents-Nicolas J, Brufau-de Barbera M, Cabratosa-Termes J. Use of polyetheretherketone in the fabrication of a maxillary obturator prosthesis: a clinical report. J Prosthet Dent. 2014;112(3):680-2.
131. Hahnel S, Scherl C, Rosentritt M. Interim rehabilitation of occlusal vertical dimension using a double-crown-retained removable dental prosthesis with polyetheretherketone framework. J Prosthet Dent. 2018;119(3):315-8.
132. Schwitalla A, Muller WD. PEEK dental implants: a review of the literature. J Oral Implantol. 2013;39(6):743-9.
133. Adell R, Eriksson B, Lekholm U, Brånemark P-I, Jemt T. A long-term follow-up study of osseointegrated implants in the treatment of totally edentulous jaws. Int J Oral Maxillofac Implants. 1990;5(4).
134. Koutouzis T, Richardson J, Lundgren T. Comparative soft and hard tissue responses to titanium and polymer healing abutments. J Oral Implantol. 2011;37 Spec No:174-82.
135. Santing HJ, Meijer HJ, Raghoebar GM, Özcan M. Fracture strength and failure mode of maxillary implant-supported provisional single crowns: a comparison of composite resin crowns fabricated directly over PEEK abutments and solid titanium abutments. Clin Implant Dent Relat Res. 2012;14(6):882-9.

136. Kjellin P, Andersson M. SE-0401524-4, assignee. Synthetic nano-sized crystalline calcium phosphate and method of production patent SE527610. 2006.
137. Albrektsson T, Wennerberg A. Oral implant surfaces: Part 1--review focusing on topographic and chemical properties of different surfaces and in vivo responses to them. Int J Prosthodont. 2004;17(5):544-64.
138. Donath K. Die trenn-dünnschliff-technik zur herstellung histologischer präparate von nicht schneidbaren geweben und materialien. Der Präparator. 1988;34(1):197-206.
139. Johansson CB, Morberg P. Importance of ground section thickness for reliable histomorphometrical results. Biomaterials. 1995;16(2):91-5.
140. Johansson CB, Morberg P. Cutting directions of bone with biomaterials in situ does influence the outcome of histomorphometrical quantifications. Biomaterials. 1995;16(13):1037-9.
141. Sarve H, Johansson CB, Lindblad J, Borgefors G, Stenport VF. Quantification of bone remodeling in the proximity of implants. Proceedings of the 12th international conference on Computer analysis of images and patterns; Vienna, Austria. 1770939: Springer-Verlag; 2007. p. 253-60.
142. Johansson CB, Roeser K, Jimbo R, Hammarström Johansson P, Larsson L, Östberg AK. 3.16 Histological Analysis☆. In: Ducheyne P, editor. Comprehensive Biomaterials II. Oxford: Elsevier; 2017. p. 335-63.
143. Christensen GD, Simpson WA, Younger J, Baddour L, Barrett F, Melton D, et al. Adherence of coagulase-negative staphylococci to plastic tissue culture plates: a quantitative model for the adherence of staphylococci to medical devices. J Clin Microbiol. 1985;22(6):996-1006.
144. Ivanoff CJ, Sennerby L, Lekholm U. Influence of initial implant mobility on the integration of titanium implants. An experimental study in rabbits. Clin Oral Implants Res. 1996;7(2):120-7.
145. Schatzker J, Horne JG, Sumner-Smith G. The effect of movement on the holding power of screws in bone. Clin Orthop Relat Res. 1975(111):257-62.
146. Wennerberg A. On surface roughness and implant incorporation [Thesis]: University of Gothenburg, Gothenburg, Sweden; 1996.
147. He W, Kjellin P, Currie F, Handa P, Knee CS, Bielecki J, et al. Formation of Bone-like Nanocrystalline Apatite Using Self-Assembled Liquid Crystals. Chem Mater. 2011;24(5):892-902.
148. Ducheyne P, Qiu Q. Bioactive ceramics: the effect of surface reactivity on bone formation and bone cell function. Biomaterials. 1999;20(23-24):2287-303.
149. Zhu X, Eibl O, Scheideler L, Geis-Gerstorfer J. Characterization of nano hydroxyapatite/collagen surfaces and cellular behaviors. Journal of biomedical materials research Part A. 2006;79(1):114-27.
150. Johansson CB, Jimbo R, Stefenson P. Ex vivo and in vivo biomechanical test of implant attachment to various materials: introduction of a new user-friendly removal torque equipment. Clin Implant Dent Relat Res. 2012;14(4):603-11.
151. Arnett TR. Extracellular pH regulates bone cell function. J Nutr. 2008;138(2):415s-8s.
152. Johansson CB, Albrektsson T, Thomsen P, Sennerby L, Lodding A, Odelius H. Tissue reactions to titanium-6aluminum-4vanadium alloy. Eur J Exp Musculoskel Res. 1992;1:161-9.

153. Thomsen P, Gretzer C. Macrophage interactions with modified material surfaces. Curr Opin Solid State Mater Sci. 2001;5(2):163-76.
154. St Pierre CA, Chan M, Iwakura Y, Ayers DC, Kurt-Jones EA, Finberg RW. Periprosthetic osteolysis: Characterizing the innate immune response to titanium wear-particles. J Orthop Res. 2010;28(11):1418-24.
155. Zhang Q, Chen B, Yan F, Guo J, Zhu X, Ma S, et al. Interleukin-10 inhibits bone resorption: a potential therapeutic strategy in periodontitis and other bone loss diseases. BioMed research international. 2014;2014:284836.
156. Heino TJ, Hentunen TA, Vaananen HK. Osteocytes inhibit osteoclastic bone resorption through transforming growth factor-beta: enhancement by estrogen. J Cell Biochem. 2002;85(1):185-97.
157. Refai AK, Textor M, Brunette DM, Waterfield JD. Effect of titanium surface topography on macrophage activation and secretion of proinflammatory cytokines and chemokines. J Biomed Mater Res Part A. 2004;70(2):194-205.
158. Chen S, Jones JA, Xu Y, Low H-Y, Anderson JM, Leong KW. Characterization of topographical effects on macrophage behavior in a foreign body response model. Biomaterials. 2010;31(13):3479-91.
159. Soskolne WA, Cohen S, Shapira L, Sennerby L, Wennerberg A. The effect of titanium surface roughness on the adhesion of monocytes and their secretion of TNF-α and PGE2. Clin Oral Implants Res. 2002;13(1):86-93.
160. Lee HS, Stachelek SJ, Tomczyk N, Finley MJ, Composto RJ, Eckmann DM. Correlating macrophage morphology and cytokine production resulting from biomaterial contact. J Biomed Mater Res Part A. 2013;101(1):203-12.
161. Johansson C, Albrektsson T, Ericson L, Thomsen P. A quantitative comparison of the cell response to commercially pure titanium and Ti-6Al-4V implants in the abdominal wall of rats. J Mater Sci Mater Med. 1992;3(2):126-36.
162. Esposito M, Hirsch JM, Lekholm U, Thomsen P. Biological factors contributing to failures of osseointegrated oral implants,(II). Etiopathogenesis. Eur J Oral Sci. 1998;106(3):721-64.
163. Manolagas S. Role of cytokines in bone resorption. Bone. 1995;17(2):S63-S7.
164. Al Saffar N, Revell P. Interleukin-1 production by activated macrophages surrounding loosened orthopaedic implants: a potential role in osteolysis. Rheumatology. 1994;33(4):309-16.
165. Trindade R, Albrektsson T, Galli S, Prgomet Z, Tengvall P, Wennerberg A. Osseointegration and foreign body reaction: Titanium implants activate the immune system and suppress bone resorption during the first 4 weeks after implantation. Clin Implant Dent Relat Res. 2018;20(1):82-91.
166. Trindade R, Albrektsson T, Galli S, Prgomet Z, Tengvall P, Wennerberg A. Bone Immune Response to Materials, Part I: Titanium, PEEK and Copper in Comparison to Sham at 10 Days in Rabbit Tibia. Journal of clinical medicine. 2018;7(12).
167. Wassmann T, Kreis S, Behr M, Buergers R. The influence of surface texture and wettability on initial bacterial adhesion on titanium and zirconium oxide dental implants. International Journal of Implant Dentistry. 2017;3(1):32.
168. Song F, Koo H, Ren D. Effects of Material Properties on Bacterial Adhesion and Biofilm Formation. J Dent Res. 2015;94(8):1027-34.
169. Auschill TM, Arweiler NB, Brecx M, Reich E, Sculean A, Netuschil L. The effect of dental restorative materials on dental biofilm. Eur J Oral Sci. 2002;110(1):48-53.

170. Quirynen M, Bollen C. The influence of surface roughness and surface-free energy on supra-and subgingival plaque formation in man: A review of the literature. J Clin Periodontol. 1995;22(1):1-14.
171. Mabboux F, Ponsonnet L, Morrier JJ, Jaffrezic N, Barsotti O. Surface free energy and bacterial retention to saliva-coated dental implant materials--an in vitro study. Colloids and surfaces B, Biointerfaces. 2004;39(4):199-205.
172. Wang A, Jones IP, Landini G, Mei J, Tse YY, Li YX, et al. Backscattered electron imaging and electron backscattered diffraction in the study of bacterial attachment to titanium alloy structure. J Microsc. 2018;270(1):53-63.
173. van Merode AE, van der Mei HC, Busscher HJ, Krom BP. Influence of culture heterogeneity in cell surface charge on adhesion and biofilm formation by Enterococcus faecalis. J Bacteriol. 2006;188(7):2421-6.
174. Shah FA, Trobos M, Thomsen P, Palmquist A. Commercially pure titanium (cp-Ti) versus titanium alloy (Ti6Al4V) materials as bone anchored implants—Is one truly better than the other? Materials Science and Engineering: C. 2016;62:960-6.
175. Hannig C, Hannig M. The oral cavity—a key system to understand substratum-dependent bioadhesion on solid surfaces in man. Clin Oral Investig. 2009;13(2):123-39.
176. Marsh P. Dental plaque as a microbial biofilm. Caries Res. 2004;38(3):204-11.
177. Sandoe JA, Witherden IR, Cove JH, Heritage J, Wilcox MH. Correlation between enterococcal biofilm formation in vitro and medical-device-related infection potential in vivo. J Med Microbiol. 2003;52(Pt 7):547-50.